

Systematics and Molecular Phylogeny of the Family Oscarellidae (Homoscleromorpha) with Description of Two New *Oscarella* Species

Eve Gazave^{1,2*}, Dennis V. Lavrov³, Jory Cabrol², Emmanuelle Renard², Caroline Rocher², Jean Vacelet², Maja Adamska⁴, Carole Borchiellini², Alexander V. Ereskovsky^{2,5}

1 Institut Jacques Monod, CNRS, UMR 7592, Université Paris Diderot, Sorbonne Paris Cité, Paris, France, **2** Aix-Marseille Université, CNRS, UMR 7263, Mediterranean Institute of Biodiversity and Ecology (IMBE), Marseille, France, **3** Department of Ecology, Evolution, and Organismal Biology, Iowa State University, Ames, Iowa, United States of America, **4** Sars International Centre for Marine Molecular Biology, Bergen, Norway, **5** Department of Embryology, Faculty of Biology and Soil Science, St-Petersburg State University, Saint-Petersburg, Russia

Abstract

The family Oscarellidae is one of the two families in the class Homoscleromorpha (phylum Porifera) and is characterized by the absence of a skeleton and the presence of a specific mitochondrial gene, *tatC*. This family currently encompasses sponges in two genera: *Oscarella* with 17 described species and *Pseudocortidium* with one described species. Although sponges in this group are relatively well-studied, phylogenetic relationships among members of Oscarellidae and the validity of genus *Pseudocortidium* remain open questions. Here we present a phylogenetic analysis of Oscarellidae using four markers (18S rDNA, 28S rDNA, *atp6*, *tatC*), and argue that it should become a mono-generic family, with *Pseudocortidium* being synonymized with *Oscarella*, and with the transfer of *Pseudocortidium jarrei* to *Oscarella jarrei*. We show that the genus *Oscarella* can be subdivided into four clades, each of which is supported by either a small number of morphological characters or by molecular synapomorphies. In addition, we describe two new species of *Oscarella* from Norwegian fjords: *O. bergensis* sp. nov. and *O. nicolae* sp. nov., and we compare their morphology, anatomy, and cytology with other species in this genus. Internal anatomical characters are similar in both species, but details of external morphology and particularly of cytological characters provide diagnostic features. Our study also confirms that *O. lobularis* and *O. tuberculata* are two distinct polychromic sibling species. This study highlights the difficulties of species identification in skeleton-less sponges and, more generally, in groups where morphological characters are scarce. Adopting a multi-marker approach is thus highly suitable for these groups.

Citation: Gazave E, Lavrov DV, Cabrol J, Renard E, Rocher C, et al. (2013) Systematics and Molecular Phylogeny of the Family Oscarellidae (Homoscleromorpha) with Description of Two New *Oscarella* Species. PLoS ONE 8(5): e63976. doi:10.1371/journal.pone.0063976

Editor: Donald James Colgan, Australian Museum, Australia

Received: October 22, 2012; **Accepted:** April 6, 2013; **Published:** May 30, 2013

Copyright: © 2013 Gazave et al. This is an open-access article distributed under the terms of the Creative Commons Attribution License, which permits unrestricted use, distribution, and reproduction in any medium, provided the original author and source are credited.

Funding: This work was supported by the Centre National de Recherche Scientifique, Aix-Marseille Université and by the National Science Foundation [DEB-0828783]. The funders had no role in study design, data collection and analysis, decision to publish, or preparation of the manuscript.

Competing Interests: The authors have declared that no competing interests exist.

* E-mail: gazave.eve@ijm.univ-paris-diderot.fr

Introduction

Sponges (phylum Porifera) are now formally regarded as being composed of four lineages: Demospongiae, Calcarea, Hexactinellida and Homoscleromorpha [1,2,3,4,5]. The latter group, Homoscleromorpha, contains about 78 species and is subdivided into two families: Plakinidae and Oscarellidae [1,6]. Currently, family Plakinidae encompasses five spiculate genera (*Plakina*, *Plakortis*, *Plakinastrella*, *Placinolopha* and *Cortidium*) while Oscarellidae includes two aspiculate genera (*Oscarella* and *Pseudocortidium*) [1,6]. Family Oscarellidae [6] was established by Lendenfeld in 1887, but was rejected in 1995 [7] following the description of *Pseudocortidium*, which is morphologically similar to *Cortidium* though lacking spicules. Oscarellidae was restored as a family only recently as the result of studies of molecular phylogeny [6] and metabolomic fingerprints [8] of Homoscleromorpha. The results of these studies have demonstrated that morphological similarities found in spiculate *Cortidium* and aspiculate *Pseudocortidium* (cortex, aquiferous system organization, and outer morphology) are either

plesiomorphic or homoplastic characters [6] and that *Pseudocortidium* is, in fact, more closely related to *Oscarella* species with very different internal and external morphology.

Although the subdivision of Homoscleromorpha into two families is now formally accepted by the sponge scientific community [1,6,9], the relationships between the two oscarellid genera and consequently, the monophyly of *Oscarella*, remain contentious. Indeed, in our previous study [6], the analyses of complete mtDNA genomes and 18S rDNA data supported the paraphyly of the *Oscarella*, which encompassed *Pseudocortidium jarrei* Boury-Esnault et al., 1995. In contrast, the 28S rDNA sequences supported the monophyly of *Oscarella* with *P. jarrei* as its sister group. In order to resolve this issue, we conducted a further molecular study including additional *Oscarella* species.

Oscarella lobularis (Schmidt, 1862) [10], the type species of the genus, was long considered to be a single abundant cosmopolitan species displaying a high polymorphism of both consistency (soft and cartilaginous) and color (purple, blue, yellow and green) [11]. In 1992, Boury-Esnault and colleagues investigated the relation-

ships among four color morphotypes of *O. lobularis* from the Marseille area by analyzing their allozymes and cytological features [12]. They showed that two species were present rather than one: *O. lobularis* (the soft purple/ivory specimens, [13]) and *O. tuberculata* (Schmidt, 1868) (the yellow, green or blue cartilaginous specimens). Since then, however, the picture has become more complex and is rife with ambiguities. Recent studies have found soft specimens of *Oscarella* which do not have the habitual purple/ivory coloring, but which are blue, entirely purple or pink. Similarly, cartilaginous specimens of *Oscarella* may also be purple or pink in addition to the green, blue and yellow morphotypes [13,14]. Subsequent, finer histological studies revealed additional differences among various color morphs of *Oscarella*, and the 'cosmopolitan' *O. lobularis* turns out to be different species (10 new species of *Oscarella* have been described during the last 20 years) [15,16,17,18]. The absence of a skeleton (the main morphological character for sponge taxonomy) and thus, the paucity of available morphological characters for *Oscarella* systematics, is largely responsible for difficulties associated with species delimitation in this genus, as well as in other genera of sponges without skeletons (e.g. *Halisarca* [19,20,21]). At present, *Oscarella* comprises 17 species, listed in the World Porifera Data Base (<http://www.marinespecies.org/porifera/index.php>), including seven Mediterranean species. However, this is certainly an underestimate and several new species are currently under description (this study) or have yet to be described. The relationships among these 17 *Oscarella* species and the phylogenetic position of *Pseudocorticium jarrei* relative to them are also largely unknown [6]. In addition, the relationships between the different color morphs of the two putative sibling species *O. lobularis* and *O. tuberculata* [14] have not yet been fully resolved and more loci from more color morphs are needed to elucidate them. This is crucially important, especially because *O. lobularis* is being developed as a new model species for evo-devo studies [13,22,23,24,25].

Thus the aim of this paper is to investigate the principal uncertainties in the phylogeny of Oscarellidae described above: (i) the position of *Pseudocorticium jarrei* and the monophyly of genus *Oscarella*, (ii) the relationships among common *Oscarella* species, (iii) the relationships between different color morphs of *Oscarella lobularis* and *O. tuberculata*. For this purpose, we collected a diverse dataset relating to 22 Oscarellidae specimens from different geographical areas. Our dataset includes four molecular markers (two nuclear (18S rDNA, 28S rDNA) and two mitochondrial (*atp6*, *tatC*)), predicted secondary structures features for nuclear rDNAs [26] and multiple non-molecular characters (in particular, histological and cytological). We also incorporated two new species of *Oscarella* from Bergen Fjords in our analysis, and we provide their morphological descriptions and formal diagnoses. We discuss our results from an integrative taxonomic point of view [27].

Methods

1. Specimen Collection

Specimens of Oscarellidae from the Mediterranean Sea, the Norwegian Fjords, the East Atlantic and the North Pacific were collected using SCUBA diving by members of our team (AVE, EG) or were provided by colleagues (see Acknowledgments). Locations of the collection sites are shown on Figure 1. The samples used in this study and their current taxonomic status are summarized in Table 1. The different color morphs of *Oscarella lobularis* and *O. tuberculata* are presented *in situ* in Figure S1. We obtained molecular data from 9 of the 17 officially described species of *Oscarella*. In addition, we formally describe two new

species in this paper and discuss two specimens with uncertain systematic positions (*Oscarella* sp. (pink) and *Oscarella* sp. (purple)). Despite substantial efforts, we did not succeed in obtaining DNA from museum specimens of *O. nigraviolacea* Bergquist & Kelly, 2004, *O. ochracea* Muricy & Pearce, 2004 and *O. stillans* Bergquist & Kelly, 2004; likely due to problems with DNA preservation [28,29]. We choose not to include in our sampling *O. imperialis* Muricy et al., 1996 [30], as we were unable to find this species with certainty *in situ*.

2. Morphological Studies

2.1. Taxonomy. The identification of all specimens has been carefully checked on the basis of morphological characters by the taxonomists in our team (AVE and JV).

2.2. Description of new species. Specimens from Norway were collected using SCUBA diving on June 23 2009 from vertical walls of granite rocks (North Sea, Norway, Skarvoysundet +60° 27' 34.74" N, +4° 56' 2.16" E) at depths of 3 to 9 m. Vouchers for transmission electron microscopy (TEM) and scanning electron microscopy (SEM) were fixed according to [31]. Sections were cut with a diamond knife on a Leica Ultracut UCT Ultramicrotome. Semi-thin sections were stained with toluidine blue, observed using light microscopy (LM) and photographed with a Leica DMLB digital camera. For SEM, the specimens were fractured in liquid nitrogen, critical-point-dried, sputter-coated with gold-palladium, and observed under a Hitachi S570 SEM. Type specimens have been deposited in the Muséum National d'Histoire Naturelle (MNHN, Paris, France) and the new species have been registered in ZooBank.

2.3. Nomenclatural Acts. The electronic edition of this article conforms to the requirements of the amended International Code of Zoological Nomenclature, and hence the new names contained herein are available under that Code from the electronic edition of this article. This published work and the nomenclatural acts it contains have been registered in ZooBank, the online registration system for the ICZN. The ZooBank LSIDs (Life Science Identifiers) can be resolved and the associated information viewed through any standard web browser by appending the LSID to the prefix "<http://zoobank.org/>". The LSID for this publication is: urn:lsid:zoobank.org:pub:**9766D4A6-D2B5-4311-BFDB-8B3262B401F1**. The electronic edition of this work was published in a journal with an ISSN, and has been archived and is available from the following digital repositories: PubMed Central and LOCKSS.

2.4. Non-molecular characters. To identify putative non-molecular synapomorphies for clades revealed by molecular analyses, several characters belonging to five major categories - (i) ecology/geography, (ii) external morphology, (iii) histology/cytology, (iv) microbiology and (v) embryology - are described for each species. Observed characters and their states are listed in Tables 2 and 3. Most of these characters are non-informative for phylogenetic reconstruction and thus this table of characters has not been used as a matrix for phylogenetic analyses. Instead, parsimony reconstruction of character evolution (the matrix of characters is provided in Text S1) based on the consensus molecular tree (Figure S2) was performed using Mesquite software version 2.72 [32].

3. Molecular Methods

3.1. Rationale for the choice of molecular markers. Our decision to use 18S rDNA and 28S rDNA markers in our analysis was based on their prior efficacy in solving phylogenetic relationships at the genus and supra-generic levels for various sponge groups [2,6,33,34,35,36,37]. In addition, we developed

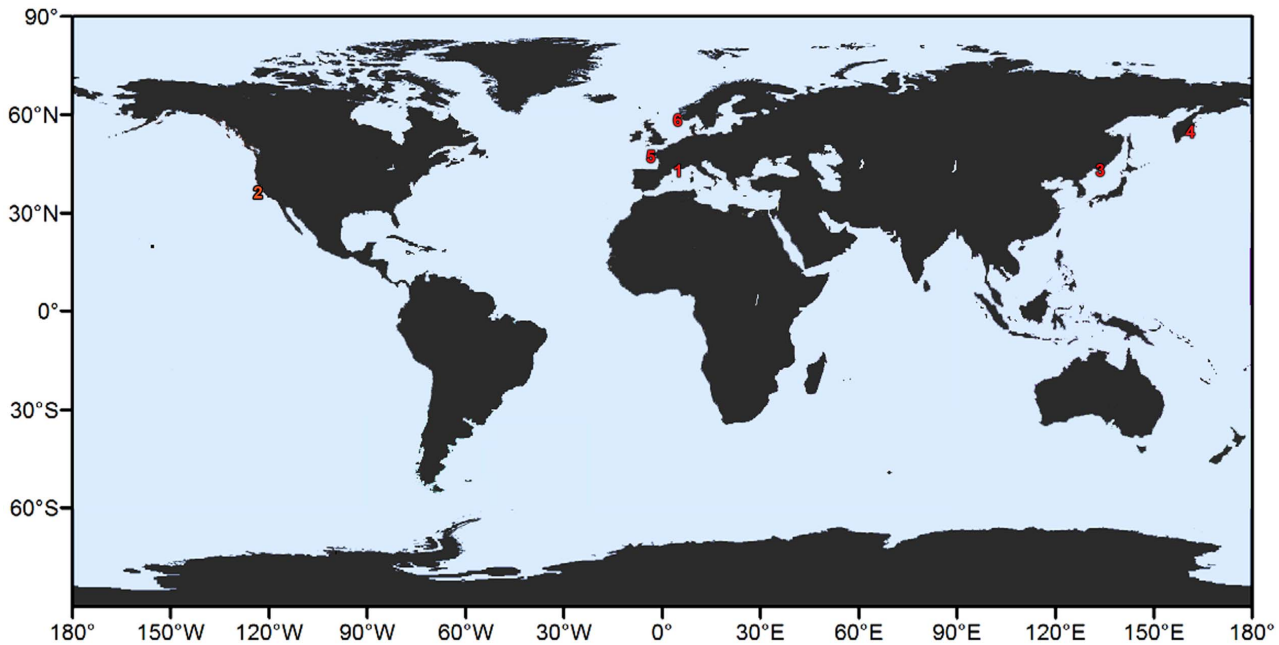


Figure 1. Map of the collection sites for this study. The numbers refer to the species locations detailed in Table 1.
doi:10.1371/journal.pone.0063976.g001

two new mitochondrial markers for Homoscleromorpha based on our previous data [6] and on new complete mtDNA sequences from *Oscarella tuberculata* yellow and *Oscarella* sp. (purple). The regions chosen for these markers are located within *tatC* and *atp6* and contain the largest number of parsimony informative sites per kb of sequence in a whole mt-genome alignment for five closely-related *Oscarella* species: *O. tuberculata* green, *O. tuberculata* yellow, *Oscarella* sp. (purple), *O. lobularis*, and *O. viridis*. Together, these two markers encompassed ~30% of such sites (10/35) in fewer than 8% of mt-genome sequences.

Interestingly, *atp6* has recently been used in another study where it has been shown to be suitable for alpha-level systematics in sponges [38]. To circumvent the pitfalls of using single-gene trees, which can tell a biased story of the species relationships [38,39], we combined these four genes in our analysis.

3.2. DNA sequence acquisition. Procedures used for genomic DNA extraction, cloning and DNA sequencing are standard laboratory protocols described in previous publications [6,37]. PCR primers for full-length/partial 18S rDNA, partial 28S rDNA, *atp6* and *tatC* amplification are provided in Table S1. It was necessary to adapt reaction conditions for each species from previous studies [6,37]; the exact conditions of amplification can be provided by the authors upon request. The poriferan origin of the sequences was checked by a BLAST search [40] against the NCBI GenBank collection (<http://www.ncbi.nlm.nih.gov/>). All new sequences/genomes were deposited in GenBank under accession numbers listed in Table 1.

3.3. Sequence alignment. To achieve a reasonable trade-off between representativeness of outgroup taxa and ease of alignment, and because our prime interests were relationships within the Oscarellidae, we restricted our sampling to Homoscleromorpha. Several species of Plakinidae (three *Corticium* and two *Plakortis* species), the sister group of Oscarellidae, were used as an outgroup. Initial sequence alignment was performed using the software MUSCLE online (<http://www.ebi.ac.uk/Tools/muscle/index.html>) [41,42], and was subsequently optimized by eye using the Bioedit Sequence Alignment Editor v5.09 [43]. Ambiguously

aligned regions were determined by Gblocks v0.91 b software [44] for nuclear markers only (mitochondrial ones were partitioned by codon position). A relaxed selection of blocks is better for short alignment [45], thus the settings were the following for the 18S rDNA [1:13; 2:13; 3:8 4:2; 5: all] and the 28S rDNA [1:13; 2:13; 3:8; 4:2; 5: all]. The treatment by Gblocks resulted in the removal of 1% and 4%, for the 18S rDNA and 28S rDNA alignments, respectively. The character exclusion sets based on Gblocks are available upon request from the corresponding author.

3.4. Phylogenetic analyses. Phylogenetic analyses were performed using maximum likelihood (ML) and Bayesian inference (BI) methods.

For ML analyses, we used the Akaike Information Criterion (AIC) in JModelTest [46] to determine the best fitting nucleotide substitution model for each data set. The following models were chosen for 18S rDNA, 28S rDNA, 18S rDNA +28S rDNA, *atp6*, *tatC*, *tatC+atp6*, 18S rDNA +28S rDNA +*tatC+atp6* datasets respectively: TIM2+G; GTR+G; TIM2+G; TPM2uf+I+G; TIM1+I; GTR+G; GTR+G. ML phylogenetic analyses were performed with PhyML software v.3 [47,48] using the previously estimated parameters. Among sites, rate heterogeneity was estimated using a discrete approximation of the gamma distribution with six rate categories. Gaps were treated as missing data and the statistical robustness of the tree topology was assessed by non-parametric bootstrap resampling (1000 replicates) [49]. Bootstrap values >80 were considered high enough to support clades in ML reconstructions.

BI analyses were performed with MrBayes 3.2.1 [50] under the best-fit evolutionary model estimated for each independent gene or partition under the AIC criterion with MrModeltest 2.3 [51]. The models selected for 18S rDNA and 28S rDNA were GTR+I+G and GTR+G, respectively. For mitochondrial markers *atp6* and *tatC*, we partitioned the dataset according to codon position and the models selected are as follows; [*atp6*_1st position: GTR+I, *atp6*_2nd position: GTR+I, *atp6*_3rd position: GTR+G]; [*tatC*_1st position: GTR+I, *tatC*_2nd position: GTR+I, *tatC*_3rd position: HKY+I].

Table 1. List of species/specimens used in this work according to the classification of Systema Porifera [89] and the recent updates added to the World Porifera Database [9].

Species/color morphs		GenBank Accession numbers				Complete mt	Collection sites	
		18S rDNA	28S rDNA	<i>atp6</i>	<i>tatC</i>		Names	Map n°
<i>Oscarella</i>								
<i>Oscarella lobularis</i> purple/ivory	[10]	HM118536	HM118549	HQ269361	HQ269361	HQ269361	Marseille, France (Coral cave)	1
<i>Oscarella lobularis</i> purple	[10]	JX462755	JX462774	JX975205	JX975192	–	Marseille, France (Passe Tiboulén)	1
<i>Oscarella lobularis</i> pink	[10]	JX462757	JX462776	JX975204	JX975191	–	Marseille, France (Passe Tiboulén)	1
<i>Oscarella lobularis</i> blue	[10]	JX462756	JX462775	JX975203	JX975190	–	Marseille, France (Passe Tiboulén)	1
<i>Oscarella tuberculata</i> yellow	[88]	–	–	JX963639	JX963639	JX963639	Marseille, France (Passe Tiboulén)	1
<i>Oscarella tuberculata</i> green	[88]	JX462761	JX462777	HQ269353	HQ269353	HQ269353	Marseille, France (La Vesse)	1
<i>Oscarella tuberculata</i> pink	[88]	JX462759	JX462779	JX975207	JX975194	–	Marseille, France (La Vesse)	1
<i>Oscarella tuberculata</i> purple	[88]	JX462758	JX462780	JX975208	JX975195	–	Marseille, France (La Vesse)	1
<i>Oscarella tuberculata</i> blue	[88]	JX462760	JX462778	–	JX975193	–	Marseille, France (La Vesse)	1
<i>Oscarella carmela</i>	[29]	EU702422	EF654519	NC_009090	NC_009090	NC_009090	California, USA (Carmel Bay)	2
<i>Oscarella malakhovi</i>	[15]	HM118537	HM118550	HQ269364	HQ269364	HQ269364	Japan Sea, Russia (Vostok Bay)	3
<i>Oscarella viridis</i>	[30]	JX462764	–	HQ269358	HQ269358	HQ269358	Marseille, France (Jarre Cave)	1
<i>Oscarella microlobata</i>	[30]	HM118538	HM118551	HQ269355	HQ269355	HQ269355	Marseille, France (Jarre Cave)	1
<i>Oscarella kamchatkensis</i>	[16]	JX462762	JX462781	JX975202	JX975189	–	Avacha Gulf, Kamchatka (Starichkov Island)	4
<i>Oscarella</i> sp. (purple)	n/a	JX462766	JX462782	JX963639	JX963639	JX963640	Marseille, France (Maire Island)	1
<i>Oscarella rubra</i>	[58]	JX462765	JX462773	JX975206	JX975197	–	Ria d'Étel, France	5
<i>Oscarella balibaloï</i>	[17]	JX462763	–	JX975198	JX975196	–	Marseille, France (Coral Cave)	1
<i>Oscarella nicolae</i> sp. nov.	–	JX462769	JX462770	JX975199	JX975186	–	Bergen, Norway (Skarvoysundet)	6
<i>Oscarella</i> sp. (pink)	n/a	JX462767	JX462772	JX975200	JX975187	–	Bergen, Norway (Skarvoysundet)	6
<i>Oscarella bergensis</i> sp. nov.	–	JX462768	JX462771	JX975201	JX975188	–	Bergen, Norway (Skarvoysundet)	6
<i>Pseudocortidium</i>								
<i>Pseudocortidium jarrei</i>	[7]	HM118539	HM118552	HQ269357	HQ269357	HQ269357	Marseille, France (Jarre Cave)	1

The collection sites and the GenBank accession numbers of the four markers and of the complete mitochondrial genomes are indicated. In the sequence column, the new sequence accession numbers are written in bold.
doi:10.1371/journal.pone.0063976.t001

Four Markov Chains were run for 2 million generations and sampled every 100 generations. The chains converged significantly and the average standard deviation of split frequencies was <0.01 at the end of the run. The trees of the early generations (5000 trees) were discarded until the probabilities reached a stable plateau (burn-in) and the remaining trees were used to generate a 50% majority-rule consensus tree. Only posterior probabilities >0.90 were considered to robustly support clades.

All trees except the *tatC* and *tatC+atp6* were rooted on Plakinidae species, the exceptions arising as the *tatC* gene is specific to Oscarellidae [6]. Based on the nuclear and *atp6* phylogenetic analyses (this study) and previous complete mitochondrial analyses [6], these trees were instead rooted on a robust internal clade. The trees were visualized and edited using FigTree v.1.3.1 [52].

3.5. Secondary structure analysis of 18S rDNA sequences and their optimization on the 18S rDNA molecular

Table 2. Three sets of non-molecular characters-states for each species/specimen: ecology/geography, external morphology and associated microbes.

Clade		Ecology/Geography		External morphology			Associated microbes
		Locality	Habitat	Color	Consistency	Surface	Density of bacteria
A	<i>O. balibaloï</i>	Med	Semi-obscure caves	White Orange	Soft mucous Slimy	Corrugated Lumpy microlobate	LMA
A	<i>O. kamchatkensis</i>	N-W Pacific	Boulders Rocks	Orange Yellow	Soft slimy	Lumpy Microlobate	LMA
A	<i>O. nicolae</i> sp. nov.	E North Sea	Rocks Algae	Ivory yellowish	Delicate mucous	Microlobate	LMA
A	<i>Pseudocorticium jarrei</i>	Med	Obscure caves	Cream	Firm Cartilaginous	Smooth Slippery Corrugate Folded	HMA
B	<i>O. viridis</i>	Med	Obscure caves	Light green	Soft fragile	Rugose	LMA
C	<i>O. malakhovi</i>	N-W Pacific	Bivalve shells Stones	Pinky Yellow	Soft slimy	Lumpy Undulated Microlobate	LMA
C	<i>O. carmela</i>	N-E Pacific	Boulders	Light brown Orange	Soft slimy	Lumpy Microlobate	LMA
D	<i>O. lobularis</i>	Med	Semi-obscure caves, Walls	Variable	Soft	Smooth	LMA
D	<i>O. tuberculata</i>	Med	Semi-obscure caves Walls	Variable	Cartilaginous	Wrinkled	LMA
D	<i>O. rubra</i>	E Atlantic	Bivalve shells Stones	Yellow Red Orange	Soft cartilaginous	Lumpy Microlobate	LMA
D	<i>O. sp. (purple)</i>	Med	Bryozoan sand bottom	Purple	Soft	Microlobate	LMA
D	<i>O. sp. (pink)</i>	E North Sea	Rocks Algae	Pink	Delicate Resilience	Smooth Small wrinkles	LMA
D	<i>O. bergenensis</i> sp. nov.	E North Sea	Rocks Algae	Red Orange	Soft	Smooth Small wrinkles	LMA
?	<i>O. microlobata</i>	Med	Obscure caves	Light brown	Soft fragile	Rugose	HMA

Clades defined by molecular data are indicated (a "?" is given for *O. microlobata* for which the position is unclear). Med: Mediterranean Sea; LMA: low microbial abundance; HMA: high microbial abundance.
doi:10.1371/journal.pone.0063976.t002

tree. The MFold server (<http://mobylye.pasteur.fr/cgi-bin/MobylyePortal/portal.py?form=mfold>) [53] was used to determine secondary structures of V4 variable regions of the 18S rDNA for all species. This region was defined as covering helix 43 [54,55]. The default settings for all parameters were used as in a previous study [37]. When multiple secondary structures were found, we chose the structure with the lowest free energy (ΔG in kcal/mol) [26]. We decomposed the rDNA secondary structures into elements (framed by different colors) and defined binary characters (*i.e.* presence/absence of each element). A matrix (Text S2) was constructed and parsimony reconstructions of character evolution were performed using Mesquite software version 2.72 [32] on the 18S rDNA molecular tree.

3.6. Sequences identity and nucleotide diversities. We investigated the percentage of molecular divergence (Table 4) on the mitochondrial marker sequences (*atp6* and *tatC*) by using the identity matrix option of the Bioedit software [43]. Nucleotide diversities (π) between *Oscarella tuberculata*, *O. lobularis*, D3 sequences, as well as congeneric species of *Oscarella*, were estimated using DnaSP 5.10 software [56] for the *atp6* marker and compared to available demosponge data [38] (Table 5).

3.7. Consensus tree and diagnostic characters. A consensus tree based on *tatC+atp6* molecular phylogenies was manually drawn to map the diverse molecular and non-molecular characters that are diagnostic of some *Oscarella* clades. All robust nodes (BP>50+ PP>0.5) were conserved. Polytomy was prioritized for weakly supported nodes (BP<50 or PP<0.5).

Results

1. Molecular Phylogenies and Analyses

1.1. Phylogenetic analyses of nuclear markers: 18S rDNA and 28S rDNA genes. The results of the analyses of 18S rDNA and 28S rDNA genes, both separate and combined are mostly congruent and are presented in Figures 2. In the following text section, the bootstraps and posterior probabilities values corresponding to a given node will be listed (in brackets) in the following order: 18S rDNA BP/PP, 28S rDNA BP/PP, 18S rDNA +28S rDNA BP/PP, when relevant. Two well-supported clades named A (81/0.87, 92/1, 96/1) and B (99/1, 97/1, 99/1) are found in these topologies.

Clade A contains *Oscarella balibaloï* Perez et al., 2011, *O. kamchatkensis* Ereskovsky et al., 2009 and *O. nicolae* sp. nov. (see description hereafter)+*Pseudocorticium jarrei*. Although we failed to obtain *O. balibaloï*'s 28S rDNA sequence, 18S rDNA and 18S rDNA +28S rDNA datasets highly support the pairs [*Oscarella nicolae* sp. nov.+*O. balibaloï*] and [*P. jarrei*+*O. kamchatkensis*] as having a sister-group relationship (98/1, 99/1 and 98/1, 83/1). Clade B contains all the other *Oscarella* species except for *Oscarella microlobata* Muricy et al., 1996 which is positioned as the sister group of B but with low support (58/0.69, –/0.53, 88/0.98).

Within clade B we recognize two well-supported clades named C (100/1, 100/1, 100/1) and D (100/1, 100/1, 100/1). Clade C contains *O. carmela* Muricy & Pearce, 2004 and *O. malakhovi* Ereskovsky, 2006. Clade D contains all color morphs of *O. lobularis*

Table 3. Histology, cytology and embryology morphological characters-states for each species/specimen.

Clade	Histology/Cytology							Embryology				
	Cortex system	Canal system	Choanocyte chambers	Archaeocyte	Vacuolar cells	Granular cells	Spherulose cells	Spherulose cells with para-crystalline inclusions	Basement membrane	Cinctoblastula larva	Multipolar ingression	Asynchronous spermatogenesis
A	<i>O. baibatoi</i>	No	Sylleibid	Eurypylous	No	1T	1T	No	1T	Yes	Yes	Yes
A	<i>O. kamchatkensis</i>	No	Sylleibid	Eurypylous	No	2T	2T	No	1T	Yes	Yes	Yes
A	<i>O. nicolae sp. nov.</i>	No	Sylleibid	Eurypylous	Yes	1T	1T	No	1T	Yes	Yes	Yes
A	<i>Pseudocorticium jamei</i>	Yes	Leuconoid	Diplodal	No	3T	3T	No	1T	Yes	Yes	Yes
B	<i>O. viridis</i>	No	Sylleibid	Eurypylous	Yes	1T	1T	No	No	Yes	Yes	Yes
C	<i>O. malakhovi</i>	No	Sylleibid	Eurypylous	Rare	1T	1T	No	No	Yes	Yes	Yes
C	<i>O. carmela</i>	No	Sylleibid	Eurypylous	Yes	1T	1T	No	No	Yes	Yes	Yes
D	<i>O. lobularis</i>	No	Sylleibid	Eurypylous	No	2T	No	No	No	Yes	Yes	Yes
D	<i>O. tuberculata</i>	No	Sylleibid	Eurypylous	Yes	1T	No	No	No	Yes	Yes	Yes
D	<i>O. rubra</i>	No	Sylleibid	Eurypylous	No	1T	1T	No	No	Yes	Yes	Yes
D	<i>O. sp. (purple)</i>	No	Sylleibid	Eurypylous	Yes	1T	1T	No	No	Yes	Yes	?
D	<i>O. sp. (pink)</i>	No	Sylleibid	Eurypylous	Rare	1T	1T	No	No	Yes	Yes	?
D	<i>O. beigenensis sp. nov.</i>	No	Sylleibid	Eurypylous	Rare	1T	1T	No	No	Yes	Yes	?
–	<i>O. microlobata</i>	No	Sylleibid	Eurypylous	No	1T	1T	1T	1T	Yes	Yes	Yes

Clades defined by molecular data are indicated. 1T: one type; 2T: two types; 3T: three types.
doi:10.1371/journal.pone.0063976.t003

Table 4. Identity values between members of clade D for mitochondrial markers.

	<i>O. tub_ blue</i>	<i>O. tub_ blue green</i>	<i>O. tub_ yellow</i>	<i>O. tub_ pink</i>	<i>O. tub_ purple</i>	<i>O. rubra</i>	<i>O. sp. (purple)</i>	<i>O. sp. (pink)</i>	<i>O. bergenensis</i>	<i>O. lob_ purple/ivory</i>	<i>O. lob_ pink</i>	<i>O. lob_ purple</i>	<i>O. lob_ blue</i>
<i>O. tub_ blue</i>	ID												
<i>O. tub_ green</i>	-/0.998	ID											
<i>O. tub_ yellow</i>	-/0.994	0.996/0.995	ID										
<i>O. tub_ pink</i>	-/0.998	1/1	0.996/0.995	ID									
<i>O. tub_ purple</i>	-/0.998	1/1	0.996/0.995	1/1	ID								
<i>O. rubra</i>	-/0.989	0.996/0.991	0.996/0.992	0.996/0.991	0.996/0.991	ID							
<i>O. sp. (purple)</i>	-/0.989	0.996/0.991	0.996/0.992	0.996/0.991	0.996/0.991	1/1	ID						
<i>O. sp. (pink)</i>	-/0.989	0.996/0.991	0.996/0.992	0.996/0.991	0.996/0.991	1/1	1/1	ID					
<i>O. bergenensis</i>	-/0.980	0.990/0.982	0.990/0.983	0.990/0.982	0.990/0.982	0.993/0.985	0.993/0.985	0.993/0.985	ID				
<i>O. lob_ purple/ivory</i>	-/0.986	0.992/0.988	0.992/0.989	0.992/0.988	0.992/0.988	0.995/0.991	0.995/0.991	0.995/0.991	0.995/0.982	ID			
<i>O. lob_ pink</i>	-/0.989	0.992/0.991	0.992/0.992	0.992/0.991	0.992/0.991	0.995/0.994	0.995/0.994	0.995/0.994	0.995/0.985	1/0.994	ID		
<i>O. lob_ purple</i>	-/0.991	0.992/0.992	0.992/0.994	0.992/0.992	0.992/0.992	0.995/0.995	0.995/0.995	0.995/0.995	0.995/0.986	1/0.995	1/0.998	ID	
<i>O. lob_ blue</i>	-/0.991	0.992/0.992	0.992/0.994	0.992/0.992	0.992/0.992	0.995/0.995	0.995/0.995	0.995/0.995	0.995/0.986	1/0.995	1/0.998	1/1	ID

The upper figure in each cell is for *atp6* and the lower for *tatC*. *O. lob*: *Oscarella lobularis*; *O. tub*: *O. tuberculata*.
doi:10.1371/journal.pone.0063976.t004

Table 5. Nucleotide diversity (π) of *Oscarella lobularis*, *O. tuberculata* and D3 members compared to Demospongiae species for the *atp6* marker.

Species	Number of sequences	Number of populations/localities	π	References
<i>Amphimedon erina</i>	3	1	0.000	[38]
<i>Chondrosia reniformis</i>	2	1	0.000	[38]
<i>Cinachyrella</i> sp.	9	3	0.017	[38]
<i>Ciona delitrix</i>	10	2	0.001	[38]
<i>Placospongia</i> aff. <i>carinata</i>	14	4	0.001	[38]
<i>Placospongia</i> aff. <i>melobesioides</i>	8	2	0.001	[38]
<i>Oscarella lobularis</i>	4	1	0.000	This study
<i>Oscarella tuberculata</i>	4	1	0.001	This study
D3 sequences	3	—	0.000	This study
<i>O. lobularis</i> + <i>O. tuberculata</i>	8	2	0.005	This study

For each species (or cluster), the number of sequences as well as of populations/localities is indicated.
doi:10.1371/journal.pone.0063976.t005

and *O. tuberculata*, plus two samples from Bergen (*Oscarella bergensis* sp. nov. (see description hereafter) and *Oscarella* sp. (pink)), a specimen from the East Atlantic (*O. rubra* (Hanitsch, 1890)) and a sample from the Mediterranean Sea (*Oscarella* sp. (purple)). Both nuclear markers failed to resolve clearly the relationships inside clade D (weak to moderate support in ML, and differences of topology between the three analyses).

Oscarella viridis Muricy et al., 1996 (for which only the 18S rDNA sequence was obtained) was placed as the sister group of clade [C+D] (76/1, 97/1, 84/0.99).

In summary, analyses of nuclear markers allow to clearly identify two main clades A and B, the latter being itself composed of two monophyletic groups: C and D. The relationships among the D clade (containing most of our samples) are not always clear and congruent, thus calling for the use of other markers (or more taxa).

1.2. Phylogenetic analyses of mitochondrial markers: *tatC* and *atp6* genes. The tree topologies obtained using the mt markers are generally congruent with those observed using the nuclear ones (Figures 3 and 4). In the following section, the bootstraps and posterior probability values corresponding to a given node will be listed (in brackets) in this order: (*tatC* BP/PP, *atp6* BP/PP, *tatC+atp6* BP/PP). The presence of the four clades (A, B, C, D) defined above is corroborated with the two mitochondrial gene fragments evolving at more rapid substitution rates (Tables 4 and 5). Indeed, all of these clades are strongly supported [A (100/1, 80/0.84, 100/1); B (98/1, 84/0.98, 100/1); C (100/1, 99/1, 100/1); D (100/1, 99/1, 100/1)].

The position of *Oscarella viridis* was resolved as either the sister group of C (in *tatC* tree, Figure 3A) or of D (*atp6* tree, Figure 3B) with moderate support in both cases (65/0.72, 77/0.84, —/0.65). In all cases, the positions observed here are not congruent with those found using nuclear markers.

Furthermore, in contrast to the results obtained with the nuclear genes, both mt markers have partly resolved the relationships between the members of the D clade. The latter can be subdivided into three sub-clades (variably supported): D1, D2 and D3. D1, containing all color morphs of *O. lobularis*, is moderately supported by the analyses of *tatC* and the combined dataset, but is not supported by *atp6* (—/0.71, not found, 84/0.97). D2, grouping all *O. tuberculata* color morphs, is recovered in the analyses of *atp6* (61/0.90) and *tatC+atp6* (83/0.97) mitochondrial datasets with moderate support. A sub-clade of *O. tuberculata* - with the exclusion of *O.*

tuberculata yellow - received better support in all analyses (93/0.73, 75/0.94, 96/0.98). Finally, D3 groups together *Oscarella* sp. (purple), *O. sp.* (pink) and *O. rubra* (95/1; not found; 96/1). Although the position of the third species from Bergen, *O. bergensis* sp. nov., was not precisely determined, we noted that with both nuclear and mt markers, it is unrelated to *Oscarella* sp. (pink). The mt combined dataset was more powerful than both nuclear markers and separated mt markers in resolving the relationships among D (Figure 4B).

1.3. Phylogenetic analyses of combined dataset of four markers. The topology obtained from the whole combined dataset is given in Figure 4C. The four main clades (A: 94/1; B: 100/1; C: 100/1; D: 100/1) as well as their interrelationships are retrieved. Among A, as in nuclear topologies, the robust clade [*Oscarella nicolae* sp. nov.+*O. balibaloï*] (100/1) is the sister group of the weakly supported clade [*Pseudocortium jarrei*+*O. kamchatkensis*] (55/0.71). *O. microlobata* is the sister group of B (95/1) and *O. viridis* is the sister group of D+C (63/0.94) as in 18S rDNA and 18S rDNA +28S rDNA topologies. As in the case for *tatC* marker, the sub-clade D3 is found, its robustness being weakly supported in ML and well supported in BI analyses (56/1).

1.4. Predicted secondary structures of 18S rDNA. The predicted secondary structures for the V4 region are presented in Figure 5. We have encoded the molecular morphology of the derived secondary structures as elements (loop, semi-loop and helix) and consider them as binary characters. For this purpose, we use a color code to map them and their appearance. The Oscarellidae species included in this study present different secondary structures, but all except one share a specific element of an internal loop and a terminal loop (in orange, absent in Plakinidae). The presence of this specific structure appears to be diagnostic of Oscarellidae. The absence of this element in *Oscarella lobularis* (purple/ivory) is a derived feature of this morph. Among clade A, *Oscarella nicolae* sp. nov. and *O. balibaloï* share the same secondary structure, with an additional element (compared to the other species of the clade): a central loop plus a helix, which is specific to this group (in black). Most of the species of clade B (C+D+*O. viridis*) share a similar secondary structure with a specific terminal element (one central loop and two helices, in dark blue). According to the parsimony principle, this element should be considered as a synapomorphy of this group, whereas three species (*O. malakhovi*, *O. sp.* (purple) and *O. tuberculata* pink) appear to have derived RNA structures. Species from clade C have an extra

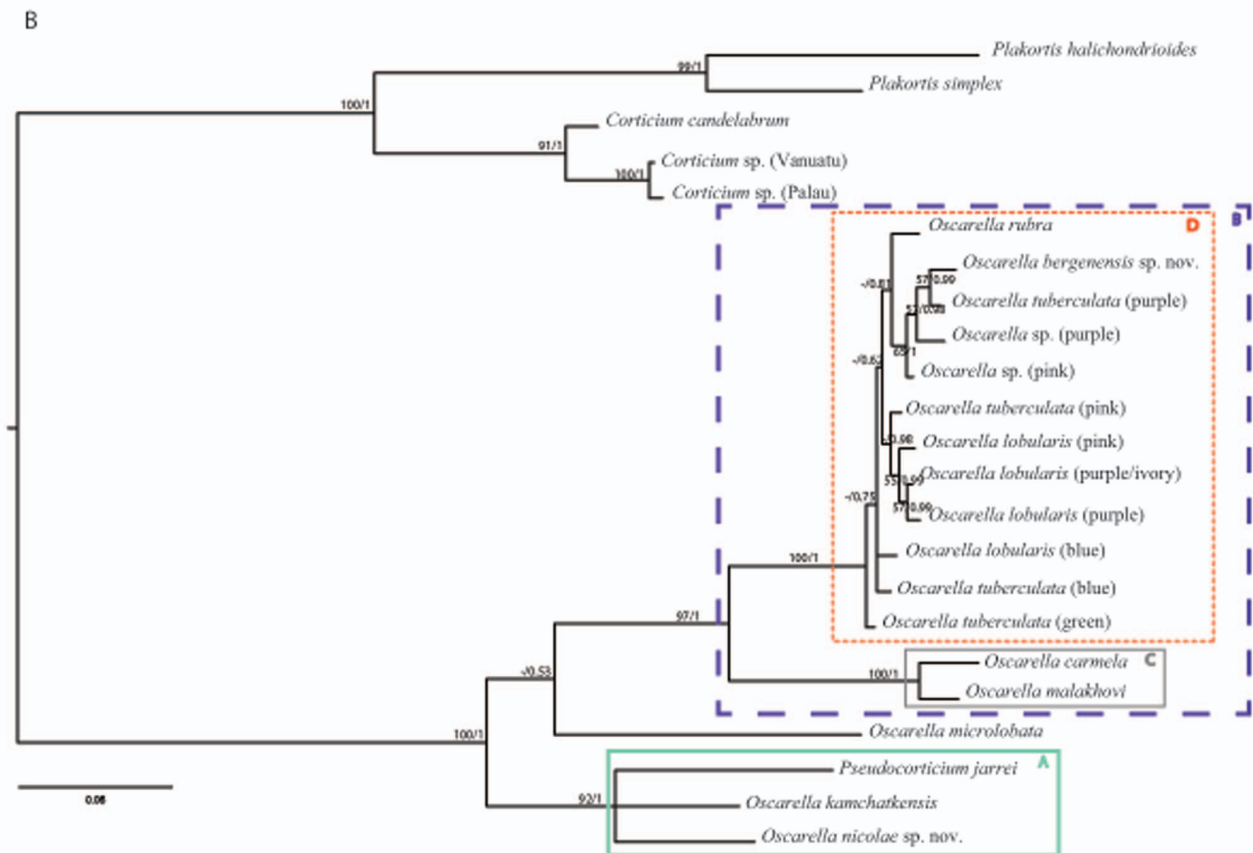
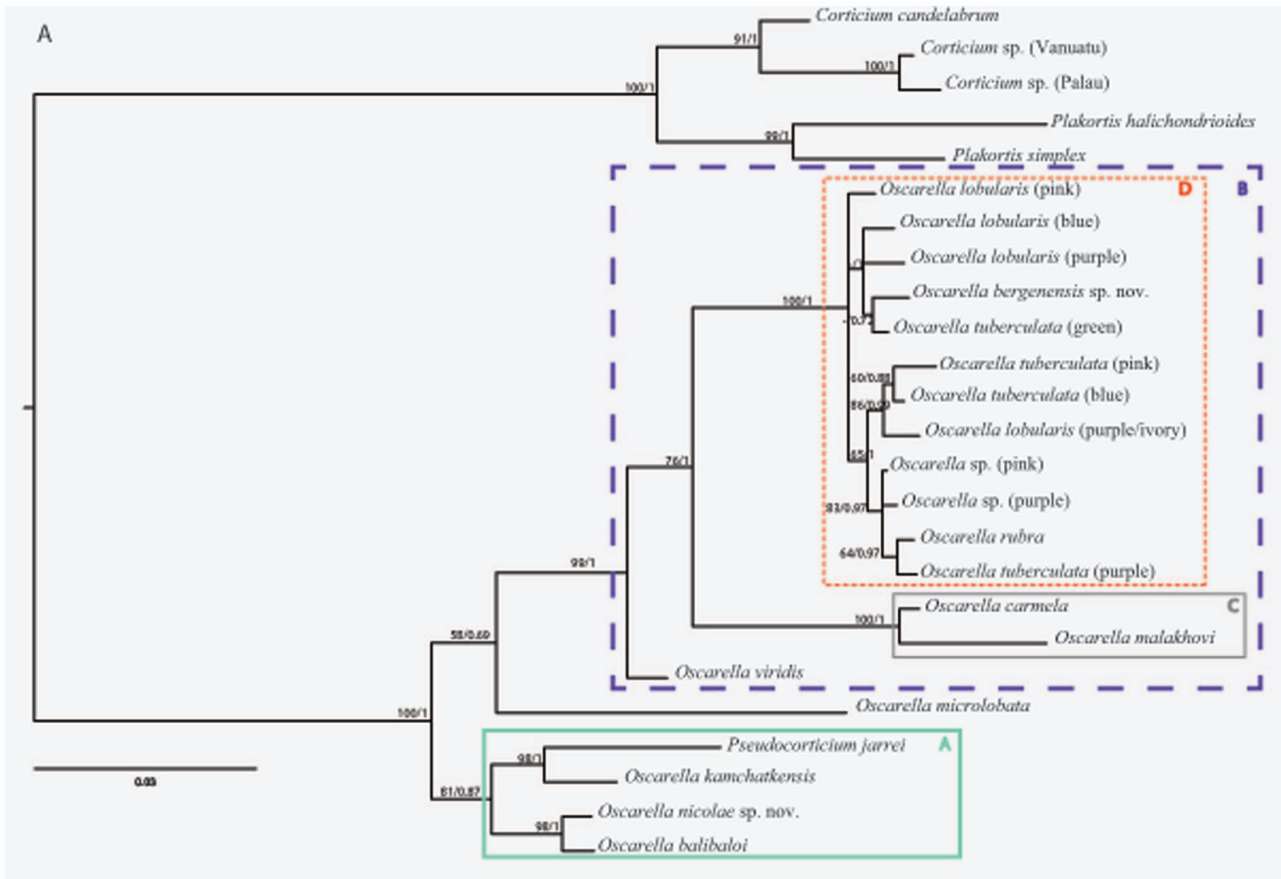


Figure 2. Phylogenetic analysis of nuclear markers. (A) 18S rDNA and (B) 28S rDNA. The topologies presented are posterior consensus trees obtained by the BI analysis using MrBayes. Similar topologies were obtained in ML analysis with PhyML. The numbers are posterior probabilities for BI and bootstrap values (>50) for ML.
doi:10.1371/journal.pone.0063976.g002

internal loop lined by three base pairs on each side (in red), which appears to be a synapomorphy of this clade. Three species from A+O. *microlobata* share a common feature (two small terminal loops, in light blue) for which no evolutionary history can be proposed.

1.5. Sequence identity, nucleotide diversity and species delimitation in Oscarellidae. Sequence identity values obtained for the mitochondrial *atp6* and *tatC* sequences for the members of clade D are presented in Table 4. The percentages of identity vary from 99.9 to 100% among *O. lobularis* (D1), from 99.4 to 100% among *O. tuberculata* (D2) and from 98 to 99.5% between the two sibling species. No differences were found for the D3 sub-clade members. *Oscarella bergenensis* sp. nov. is 98.6 to 99.4% similar when compared to the other D members. The *atp6* nucleotide diversity (π) calculation for *O. lobularis* sequences (all color morphs taken together), *O. tuberculata* (all color morphs taken together), *Oscarella* congeneric species (all color morphs for *O. lobularis* and *O. tuberculata* taken together) and D3 sub-clade members are presented in Table 5. Π values for *O. lobularis* (0.000) and *O. tuberculata* (0.001) are low and similar to those obtained for most of Demospongiae while they are five times higher when all sequences from the two congeneric species are taken together.

2. Morphological Descriptions and Systematic Justification for Two New Species

According to molecular data, it appears that at least two *Oscarella* samples from Bergen can be considered as distinct species (see discussion), and are thus morphologically and formally described herein.

Phylum PORIFERA Grant, 1836.

Class HOMOSCLEROMORPHA Bergquist, 1978.

Order HOMOSCLEROPHORIDA Dendy, 1905.

Family OSCARELLIDAE Lendenfeld, 1887.

Genus *Oscarella* Vosmaer, 1887.

TYPE SPECIES: *Halisarca lobularis* Schmidt, 1862 (by monotypy). [*Oscaria*] Vosmaer, 1881:163 (preocc. by *Oscaria* Gray, 1873– Reptilia); *Oscarella* Vosmaer, 1884: pl. 8 (explanation); 1887:326 (nom. nov. for *Oscaria* Vosmaer). *Octavella* Tuzet and Paris, 1964:88.

DIAGNOSIS (modified from [57]): Homoscleromorpha without skeleton, with a variable degree of ectosome development. The aquiferous system has a sylleibid-like or leuconoid organization, with euryplous or diplodal choanocyte chambers. Their mitochondrial genomes encode a gene absent in other animal mitochondrial genomes: *tatC*.

Oscarella Bergenensis sp. nov

TYPE MATERIAL: Holotype: MNHN DJV153, LSID:urn:l-sid:zoobank.org:act:2D44BCFA-2163-47C7-9E70-EF6-C13E0E4A4, North Sea, Norway, Bergen Fjords, Skarvoysundet +60° 27' 34.74" N, +4° 56' 2.16" E; 3–10 m depth. Collected by Alexander Ereskovsky and Marcin Adamski, 23.06.2009. Paratype: MNHN DJV154. Same data as holotype.

COMPARATIVE MATERIAL EXAMINED: *Oscarella nicolae* sp. nov. (this study), *Oscarella nathaliae* Ereskovsky, Lavrov, Willenz, 2013 (RBINS POR 90, RBINS POR 91, RBINS POR 92 and RBINS POR 94: Caribbean Sea: S Martinique, N Jamaica, Guadeloupe) [18]. *Oscarella malakhovi* Ereskovsky, 2006 (ZIN RAS 10697 ZIN RAS 10698: Japan Sea) [15]. *Oscarella kamchatkensis* Ereskovsky, Sanamyan & Vishnyakov, 2009 (ZIN

RAS 11058, ZIN RAS 11059 and ZIN RAS 11060: East-North Pacific, Avacha Gulf) [16]. *Oscarella lobularis* (Schmidt, 1862) [10], *Oscarella tuberculata* (Schmidt, 1868), NW Mediterranean Sea (Marseille region). *Oscarella microlobata* Muricy, Boury-Esnault, Bézac, Vacelet, 1996 [30], *Oscarella viridis* Muricy, Boury-Esnault, Bézac, Vacelet, 1996 [30], *Oscarella balibaloï*, Pérez, Ivanišević, Dubois, Pedel, Thomas, Tokina, Ereskovsky, 2011 [17] NW Mediterranean Sea (Marseille region).

DIAGNOSIS: Red-orange *Oscarella* at the apical parts and patchy yellow at the basal parts, with folded surface and average resilience consistency; containing two particular cell types with inclusions (vacuolar and granular cells), archaeocytes in low number in the mesohyl and one morphotype of endobiotic bacteria.

DESCRIPTION: Moderately large, encrusting, size from 2x1 cm to 6x4 cm, thickness 4–8 mm. Easy to detach from its substrate. Smooth surface but with small folds. Oscula at the end of small conical lobes 2–3 mm in height, not transparent. Consistency: average resilience. Color *in vivo* red-orange at the apical parts of sponge and patches of yellow and orange in inner parts, not bright (Figure 6A).

SOFT TISSUE ORGANISATION: Spicule and fiber skeleton absent. Ectosome from 9 to 20 μ m thick (Figure 6B). Inhalant canals (12 μ m in diameter) running perpendicular to the surface (Figure 6B). Choanocyte chambers are euryplous, roughly spherical to ovoid, about 32 μ m in diameter (Figure 6B). Choanocyte chambers are arranged around inhalant and exhalant canals in a sylleibid pattern. Exhalant canals about 40 μ m in diameter running toward well-developed system of basal cavities, leading to the oscula. Ostia regularly distributed, 16–21 μ m in diameter.

CYTOLOGY: Exopinacocytes (Figure 6C) are flat (7.1 μ m wide by 1.9 μ m high), flagellated. Nucleus is ovoid (1.6 μ m in diameter), often with a visible nucleolus. Cytoplasm contains inclusions, phagosomes (from 0.2 to 0.8 μ m in diameter) and vacuoles (0.1–0.9 μ m in diameter). Endopinacocytes (Figure 6D) are flat (7.9 μ m wide by 2.4 μ m high), flagellated, often with thin cytoplasm projections in their basal part. Nucleus is ovoid (2.2 μ m). Cytoplasm contains numerous osmiophilic inclusions as well as phagosomes (from 0.3 to 0.9 μ m in diameter) and vacuoles (0.1–1.1 μ m in diameter). Apopylar cells (Figure 6E) are triangular in section (5.2 μ m wide and 3.2 μ m high). They are flagellated with a crest of microvilli. Nucleolated nucleus is basal, ovoid, up to 2 μ m in diameter. Cytoplasm contains phagosomes and small osmiophilic inclusions. Choanocytes have irregular, pyramidal to trapeziform shape (3.4–4.7 μ m wide and 4.9–6.1 μ m high) (Figure 6F). Nucleus is central or basal, ovoid (about 2.1 μ m in dimension), often with a nucleolus. Cytoplasm usually contains phagosomes (0.5–1.5 μ m in diameter) and electron transparent vacuoles (0.18–1.0 μ m). The adjacent choanocytes are in contact with each other at their basal parts. A thin, irregular layer of glycocalyx covers the surface of exopinacocytes, endopinacocytes, choanocytes and apopylar cells. Choanoderm and pinacoderm are lined with a basement membrane, which is a continuous, 15–25 nm thick layer of condensed collagen microfibrils (Figure 6C, D, F). Archaeocytes (Figure 6G) are amoeboid, (5.6 μ m wide by 3.3 μ m length), dispersed in low number in the mesohyl. Cytoplasm includes small phagosomes, rare electron transparent vacuoles from 0.2

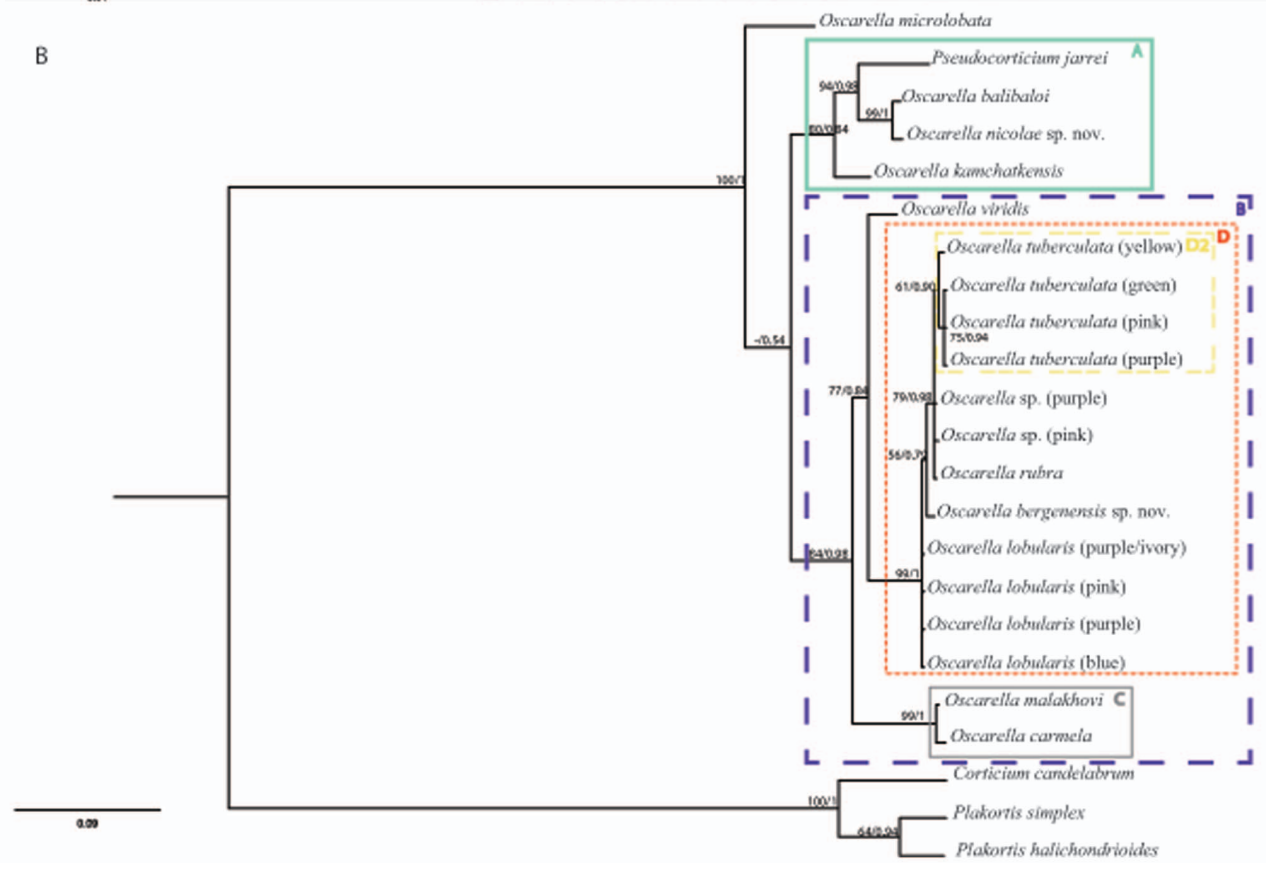
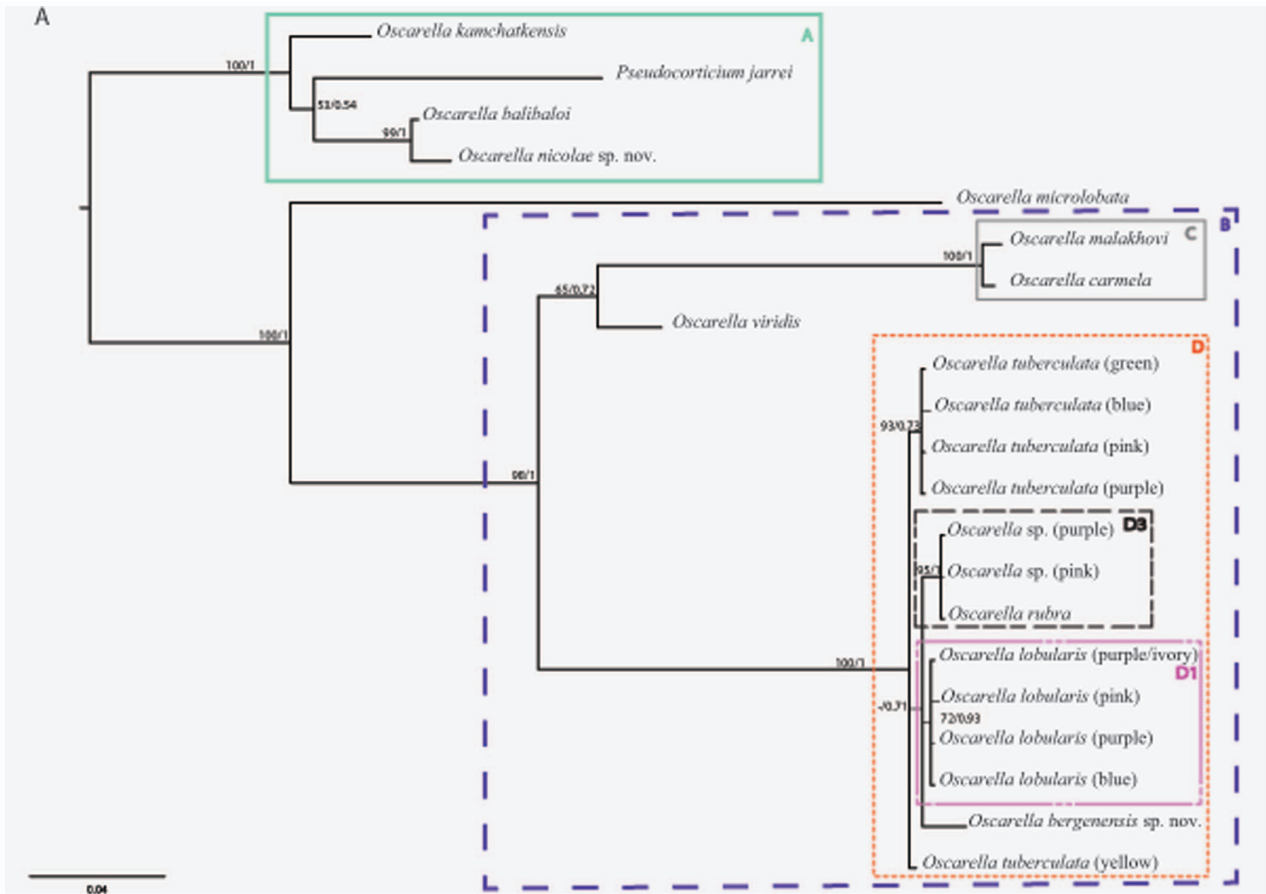


Figure 3. Phylogenetic analysis of mitochondrial markers. (A) *atp6* and (B) *tatC*. The topologies presented are posterior consensus trees obtained by the BI analysis using MrBayes. Similar topologies were obtained in ML analysis with PhyML. The numbers are posterior probabilities for BI and bootstrap values (>50) for ML.
doi:10.1371/journal.pone.0063976.g003

to 1.1 μm in diameter and rare osmiophilic inclusions, from 0.2 to 0.8 μm in diameter. A large nucleolated nucleus is spherical or ovoid, 2.2 μm in diameter. Two types of cells with inclusions are numerous within the mesohyl: Vacuolar cells (Figure 6H) are ovoid to irregular, 6.4 to 8.8 μm long with ovoid or slightly irregular nucleus 1.9 μm in diameter without nucleolus. Their cytoplasm has one to four large, irregular vacuoles (about $1.1 \times 1.6 \mu\text{m}$ to $4.1 \times 5.2 \mu\text{m}$) with clear, filamentous contents. Vacuoles are often brought together. Granular cells (Figure 6I) are ovoid to irregular (7.8 μm long and about 4.4 μm width). The nucleus is 2.2 μm in diameter. Cytoplasm is filled with 10 to 16 electron-transparent spherical vacuoles about 0.8 μm in diameter with loosely dispersed material. Rare electron-dense homogenous granules (0.4–0.9 μm in diameter) are present in the cytoplasm. Symbiotic bacteria belonging to a single morphotype are dispersed extracellularly in the mesohyl (Figure 6J). They are elongated, rod-like (length 1.1–1.8 μm and diameter 0.25–0.35 μm). The cell wall is Gram-negative and consists of two layers. A filamentous network of the nucleoid is irregular with thick elements in the center and thin filaments closer to the periphery of the cell. A small layer of granular cytoplasm is observed near the cytoplasm membrane. Short, radially-arranged filaments are present outside the cytoplasmic membrane.

REPRODUCTION: Only rare early oocytes (before vitellogenesis) were observed in the material (collected from mid- to late June).

HABITAT: Depth 3–10 m; abundant as epiphyte on the basal parts of thalli of *Laminaria digitata*, on granite rock, vertical walls.

ETYMOLOGY: The species name is derived from the site where it was discovered (Bergen fjords).

TAXONOMIC REMARKS: Regarding color, *Oscarella bergensis* sp. nov. is unusual: red-orange at the apical parts with patches of yellow at the inner parts. This coloring is almost unique compared to all described *Oscarella* species: only some specimens of *O. rubra* [58] from Roscoff have the same color pattern (AE, personal observation). The surface of *O. bergensis* sp. nov. is smooth with small folds, and is thus similar to that of *O. rubra*. Cells with inclusions of the mesohyl are important discriminating characters in *Oscarella* taxonomy. These cells are diverse and abundant in *Oscarella* species, each species being characterized by a distinctive set of cells with highly variable inclusion types [12,15,16,17,29,59]. The total cell composition and ultrastructure of *O. bergensis* sp. nov. differs from all other Mediterranean and Pacific *Oscarella* species (Table 3). *O. bergensis* sp. nov. does have a vacuolar cell very similar to those of *O. microlobata*, *O. carmela* and *O. balibalo* [17,29,30]. However, the granular cells of *O. bergensis* sp. nov. are quite different from the cells of this type described in *O. microlobata*, and *O. balibalo*, and also in *O. carmela*, *O. malakhovi*, *O. viridis* and *O. (=Pseudocorticium) jarrei*. *O. bergensis* sp. nov. shares the presence of archaeocytes with *O. viridis*, *O. carmela*, *O. malakhovi*, *O. tuberculata* and *O. nicolae* sp. nov.

Oscarella nicolae sp. nov

TYPE MATERIAL: Holotype: MNHN DJV155, LSID urn:lsid:zoobank.org:act:DFAD94B-9CAD-4F99-994D-BDE-F75EF98A1, North Sea, Norway, Bergen Fjords, Skarvøysundet +60° 27' 34.74" N, +4° 56' 2.16" E; 3–10 m depth. Collected by

Alexander Ereskovsky and Marcin Adamski, 23.06.2009. Paratype: MNHN DJV156. Same data as holotype.

COMPARATIVE MATERIAL EXAMINED: *Oscarella bergensis* sp. nov. (this study), *Oscarella nathaliae* Ereskovsky, Lavrov, Willenz, 2013 (RBINS POR 90, RBINS POR 91, RBINS POR 92 and RBINS POR 94: Caribbean Sea: S Martinique, N Jamaica, Guadeloupe) [18]. *Oscarella malakhovi* Ereskovsky, 2006 (ZIN RAS 10697 ZIN RAS 10698: Japan Sea) [15]. *Oscarella kamchatkensis* Ereskovsky, Sanamyan & Vishnyakov, 2009 (ZIN RAS 11058, ZIN RAS 11059 and ZIN RAS 11060: North Pacific, Avacha Gulf) [16]. *Oscarella lobularis* (Schmidt, 1862) [10], *Oscarella tuberculata* (Schmidt, 1868), NW Mediterranean Sea (Marseille region). *Oscarella microlobata* Muricy, Boury-Esnault, Bézac, Vacelet, 1996 [30], *Oscarella viridis* Muricy, Boury-Esnault, Bézac, Vacelet, 1996 [30], *Oscarella balibalo*, Pérez, Ivanišević, Dubois, Pedel, Thomas, Tokina, Ereskovsky, 2011 [17] NW Mediterranean Sea (Marseille region).

DIAGNOSIS: Thinly encrusting *Oscarella*, ivory-yellowish, not bright in colour, with microlobate surface and soft, delicate, slimy consistency and abundance of mucus; containing two distinct cell types with inclusions (granular cells and spherulous cells with paracrystalline inclusions), abundant archaeocytes and one morphotype of endobiotic bacteria.

DESCRIPTION: A thinly encrusting sponge, covering surface areas up to 2 cm^2 in area to thicknesses of 1.5–3 mm (Figure 7A). The sponge is very difficult to detach from the substratum. The surface is microlobate. Oscula are at the end of cylindrical tubes up to 3 mm high, transparent. Consistency: not resilient, very soft and fragile. Abundance of mucus. Color *in vivo* ivory-yellowish, not bright.

SOFT TISSUE ORGANISATION: Sponge lacks spicule and fiber skeleton. Ectosome from 10 to 20 μm thick. Inhalant canals with diameter about 25 μm run perpendicular to the surface (Figure 7B). Exhalant canals run toward a system of basal cavities, leading to the oscula. Choanocyte chambers ovoid to spherical, euryphilous about 50 μm in diameter (Figure 7B, C). The aquiferous system has a sylleibid-like organization. Ostia are 8–12 μm in diameter and regularly distributed.

CYTOLOGY: Exopinacocytes (Figure 7D) are flat to lens-like, flagellated, about 7.4 μm wide by 3.2 μm high. They are anchored in the mesohyl by long thin basal pseudopodia. Nucleus is ovoid (2.3 μm in diameter), often with a nucleolus. Cytoplasm contains inclusions and phagosomes from 0.4 to 1.3 μm in diameter. Endopinacocytes (Figure 7E) are flat, flagellated, about 9.2 μm wide by 2.3 μm high, often showing irregular, thin cytoplasm projections in their basal part. Nucleus is ovoid (1.6 \times 2.7 μm). Cytoplasm contains numerous osmiophilic inclusions and phagosomes 0.6–1.1 μm in diameter.

Apopylar cells (Figure 7F) are roughly triangular in section (7.5–9.2 μm high and 4.2–5.7 μm wide). The cells have small lateral pseudopodia. The nucleus is nucleolated, apical, ovoid, up to 2.2 \times 3 μm in cross-section. Cytoplasm contains phagosomes and small osmiophilic inclusions. Choanocytes have irregular, pyramidal to prismatic cell bodies (4.6 μm wide at the central part and 9.1 μm high) (Figure 7G). Nucleus is central or apical, ovoid (2.1 \times 3.9 μm in dimension), often with a nucleolus. Cytoplasm usually contains phagosomes (0.6–1.6 μm in diameter), smaller digestive vacuoles and osmiophilic inclusions. The adjacent choanocytes are in contact with each other at their central or

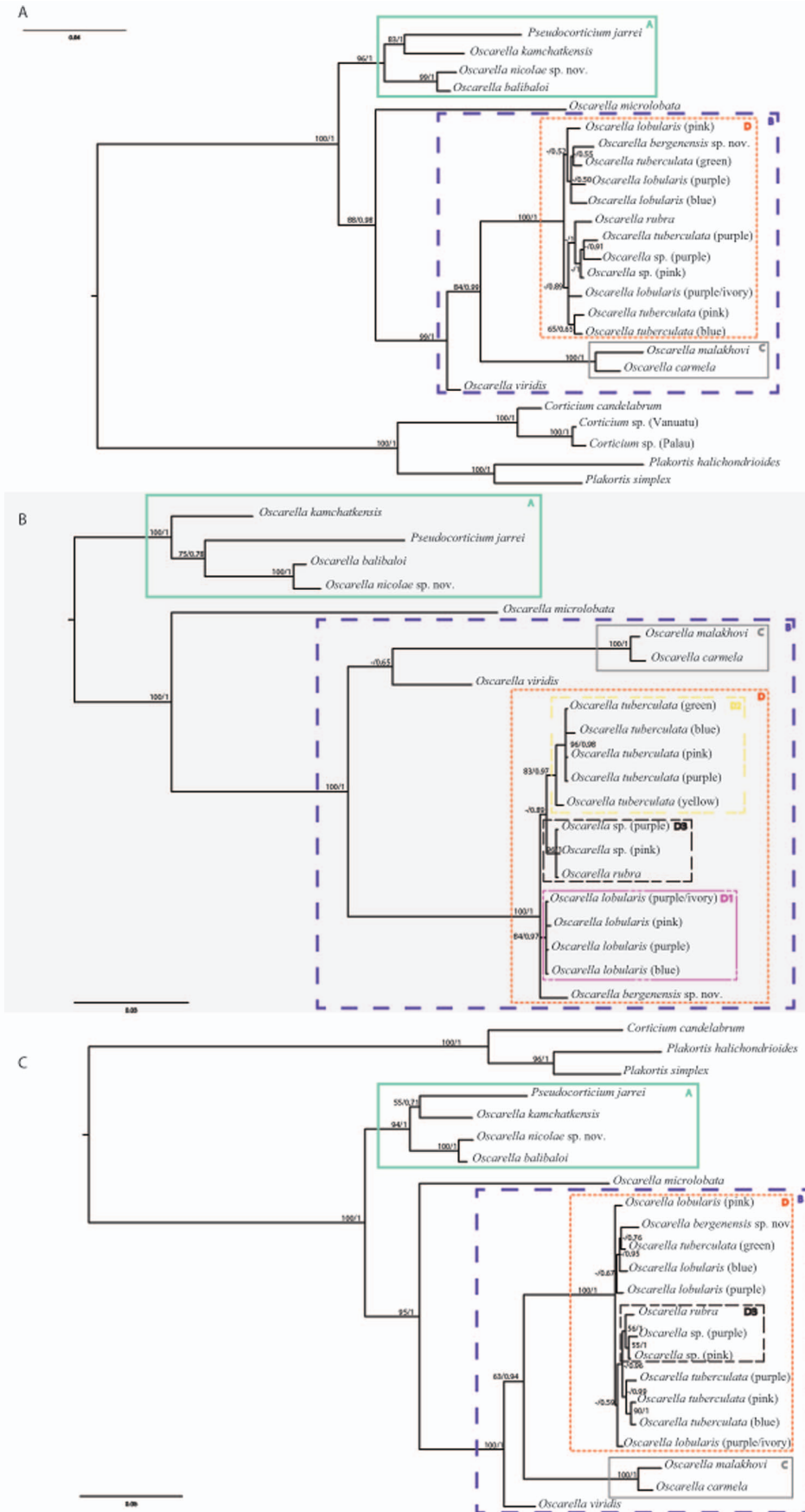


Figure 4. Oscarellidae relationships based on the analyses of concatenated sequences. (A) 18S rDNA +28S rDNA nuclear markers, (B) *atp6+ tatC* mitochondrial markers and (C) nuclear (18S rDNA +28S rDNA)+mitochondrial (*atp6+ tatC*) markers. The topologies presented are posterior consensus trees obtained by the BI analysis using MrBayes. Similar topologies were obtained in ML analysis with PhyML. The numbers are posterior probabilities for BI and bootstrap values (>50) for ML.
doi:10.1371/journal.pone.0063976.g004

basal parts. The cells have short pseudopodia. Choanoderm and pinacoderm are lined with a basement membrane, which is a continuous, 12–19 nm thick layer of condensed collagen microfibrils (Figure 7D, E, F). A thin, irregular layer of glycocalyx covers the surface of exopinacocytes, endopinacocytes, choanocytes and apopylar cells. Archaeocytes (Figure 7H) are amoeboid (7.7 μm wide by 5.1 μm length). A large nucleolated nucleus is spherical or ovoid (3.8 \times 2.9 μm). Cytoplasm includes small phagosomes and rare electron-transparent vacuoles (from 0.6 to 1.6 μm in diameter). Two types of cells with inclusions occur within the mesohyl: (i) Granular cells (Figure 7I): ovoid, 7.4 μm long and about 5.9 μm in diameter. The nucleus is 2.3 μm in diameter. Cytoplasm is filled with 6 to 12 electron dense homogenous granules, 0.6–1.2 μm in diameter. In the cytoplasm, there are some electron-transparent vacuoles (0.5–2.2 μm in diameter). Other special inclusions are absent. (ii) Spherulous cells with paracrystalline inclusions (Figure 7J): ovoid or rarely spherical cells 7.1 μm long and 5.5 μm in diameter with nucleolated nucleus 2.2 μm in diameter. Cytoplasm is filled with 5–9 spherical heterogeneous inclusions (0.9–3.2 μm in diameter), composed of paracrystalline elements included in a homogenous matrix. Paracrystalline elements are ovoid or cylindrical in longitudinal section and round in transversal section (0.7 μm long and 0.35 μm in diameter). These elements are composed of fibrils arranged in a transverse banding pattern with dark bands alternated by clear bands. In cross sections, the paracrystalline elements are organized in spiral lines. Cytoplasm can also contain 4–8 spherical granules (0.5–1.1 μm) with electron-dense homogenous inclusions and electron transparent vacuoles (0.7–1.7 μm in diameter). These cells concentrate around the eggs and are located inside them after the closing of follicle (Figure 7C). The cells are present during embryogenesis inside the embryos (Figure 7C). Symbiotic bacteria: One morphological type of endosymbiont, extracellular bacteria occurs in the mesohyl (Figure 7D, H, K). This type of bacteria is elongated to oval (0.8–1.5 μm long and 0.37–0.8 μm in diameter). Under the cell wall a layer of dense filaments can be observed. The nucleoid zone consists of an almost regular filamentous network. Some bacteria have internal mesosome-like structures. A developed glycocalyx is present at the surface of bacteria.

REPRODUCTION: *Oscarella nicolae* sp. nov. is ovoviviparous and simultaneously hermaphrodite: in the same individuals male and female reproductive elements are present. The spermatid cysts have different diameters (from 20 to 95 μm) and are randomly distributed in the sponge mesohyl (Figure 7C). Spermatogenesis is generally asynchronous inside spermatid cysts. Oogenesis and embryogenesis are asynchronous, all stages from oogonia to egg were observed within the same specimen. Mature eggs are isolecithal and polyolecithal, with a cytoplasm full of yolk granules (Figure 7C). Embryogenesis is also asynchronous. All stages from cleaving embryos to prelarva were observed from mid-June to mid-July (Figure 7C). Eggs and embryos are located in the basal part of the choanosome and are completely surrounded by a follicle made of endopinacocytes.

HABITAT: Depth 3–10 m, common and abundant as epiphyte on the basal parts of thalli of *Laminaria digitata*, on granite rock, vertical walls.

ETYMOLOGY: This species is named in honour of Dr Nicole Boury-Esnault, a remarkable taxonomist and biologist of sponges, who first drew the attention to the great diversity of *Oscarella*.

TAXONOMIC REMARKS: The ivory-yellowish color of *Oscarella nicolae* sp. nov. is not unique, but very rare in other *Oscarella*. For example, some individuals of *O. balibalo* and *O. tuberculata* from the Mediterranean Sea can also display this color. *O. nicolae* sp. nov. shares its soft consistency with *O. viridis* and *O. balibalo*, and the aspect of its surface with *O. microlobata*, *O. kamchatkensis* and *O. balibalo*. The soft slimy delicate consistency with abundant mucus, characteristic of *O. nicolae* sp. nov. differs significantly from *O. bergensis* sp. nov. The cell composition and ultrastructure of *O. nicolae* sp. nov. differ from all other Mediterranean and Pacific *Oscarella* species (Table 3). Among the two secretory cell types of the mesohyl of *O. nicolae* sp. nov., the spherulous cells with paracrystalline inclusions are very similar to the spherulous cells of *O. (=Pseudocorticium) jarrei*, *O. microlobata* (type II), *O. imperialis* (type I), *O. kamchatkensis* (type I) and *O. balibalo* (type 1) [7,16,17,30]. The granular cells of *O. nicolae* sp. nov. are similar to those of *O. kamchatkensis*. This species shares the presence of archaeocytes with *O. viridis*, *O. carmela*, *O. malakhovi*, *O. tuberculata* and *O. bergensis* sp. nov. One of the important differences between the two new species is their period of reproduction: *O. bergensis* sp. nov. contained only young oocytes in mid-June to mid-July, whereas *O. nicolae* sp. nov. is hermaphroditic with simultaneous gametogenesis (oogenesis and spermatogenesis) and embryogenesis during the same period.

3. Evolutionary Histories of Non-molecular Characters

The ecological, morphological, cytological, and embryological characters of Oscarellidae species examined in this study are presented in Tables 2 and 3.

Some of the cytological characters mentioned in these tables have often been mislabeled in previous publications and need to be clarified. According to the Thesaurus of Sponge Morphology [60] spherulous cells are cells filled with large round spherules that occupy almost the entire cytoplasm. Unfortunately, *Oscarella*'s cytology descriptions in publications are sometime ambiguous. Indeed, the cell type designations used are confusing especially concerning granular, spherulous and globular cell terms. For our analysis, we did a complete revision of previously published descriptions and photos of *Oscarella* spp., as well as a comparative analysis of TEM pictures from our collection. The results of this analysis are provided in Table 3. Spherulous cell type was described in six *Oscarella* spp.: *O. balibalo*, *O. imperialis*, *O. kamchatkensis*, *O. microlobata*, *O. (=Pseudocorticium) jarrei* and *O. nicolae* sp. nov. [7,16,17,30]. In all these species, spherulous cells have characteristic paracrystalline inclusions which have never been described in other homoscleromorphs and which are very uncommon in other sponges. Furthermore, one additional type of spherulous cell "with granular inclusions" and without paracrystalline elements was described in *O. microlobata* [30].

Evolutionary histories of characters were examined and some were found to be not informative, as they were constant in all sampled specimens (Figure S2A). This is the case for the basement membrane and several embryological characters that are present in all Homoscleromorpha. Other characters are highly variable in each species, and thus contain little phylogenetic signal. None of

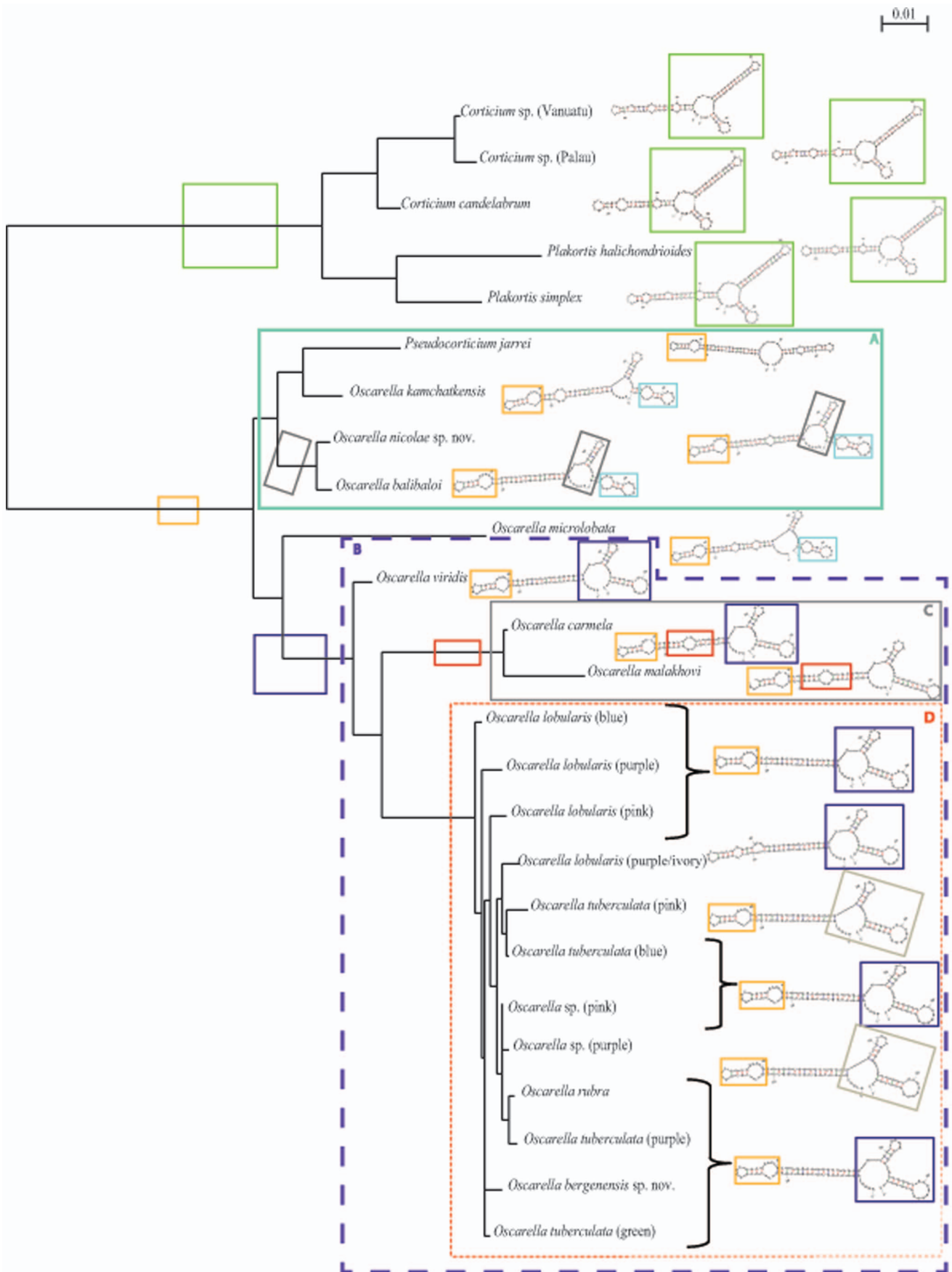


Figure 5. Schemas of the secondary structure predictions of the 18S rDNA V4 region mapped on the 18S rDNA tree topology. Elements composing the structures and included in the characters matrix are circled in a specific color. Characters that can be considered as synapomorphies are mentioned next to the corresponding node.
doi:10.1371/journal.pone.0063976.g005

the recorded ecological, geographical and external morphological characters reflects phylogenetic relationships of *Oscarella* species. Furthermore, no color, type of consistency or sort of surface can be linked to any molecular clade. Nine histological and cytological characters were compared. It is noteworthy that one cytological character, the presence of spherulous cells with paracrystalline inclusions, is found in clade A species and also in *O. microlobata* which has an unclear position in phylogenetic analyses (Figure S2B). Three characters, concerning the aquiferous system and the cortex, are constant for all but one species: *Pseudocorticium jarrei*, now *Oscarella jarrei*, which has character-states similar to the Plakinidae (outgroup) (Figure S2C). The sylleibid aquiferous system and the eurypylous choanocyte chambers appear diagnostic for Oscarellidae, however, these characters have also been described in some *Plakina* species (Plakinidae): *P. trilopha*, *P. monolopha*, *P. crypta*, *P. endoumensis*, *P. jani* [61]. In addition, we also looked at four other cellular types (archaeocytes, vacuolar cells, granular cells and spherulous cells). For the most part, their

absence or presence in different states cannot be related to any relationship supported by molecular data (Figure S2D). Nevertheless, we noticed that the vacuolar cells are absent in all clade A species with the exception of *O. balibaloii*. Our analysis suggests that the ancestral state for A members is the “absence” of vacuolar cells and that the state of *O. balibaloii* is due to reversal. In conclusion, we found very few morphological and cytological diagnostic characters supporting the clades defined based on molecular data. Clade A appears to be characterized by the absence of vacuolar cells and the presence of spherulous cells with paracrystalline inclusions, but with the exceptions of *O. balibaloii* (the member of the clade having vacuolar cells) and of *O. microlobata* (outside clade A - although with a poorly defined position - and having spherulous cells with paracrystals).

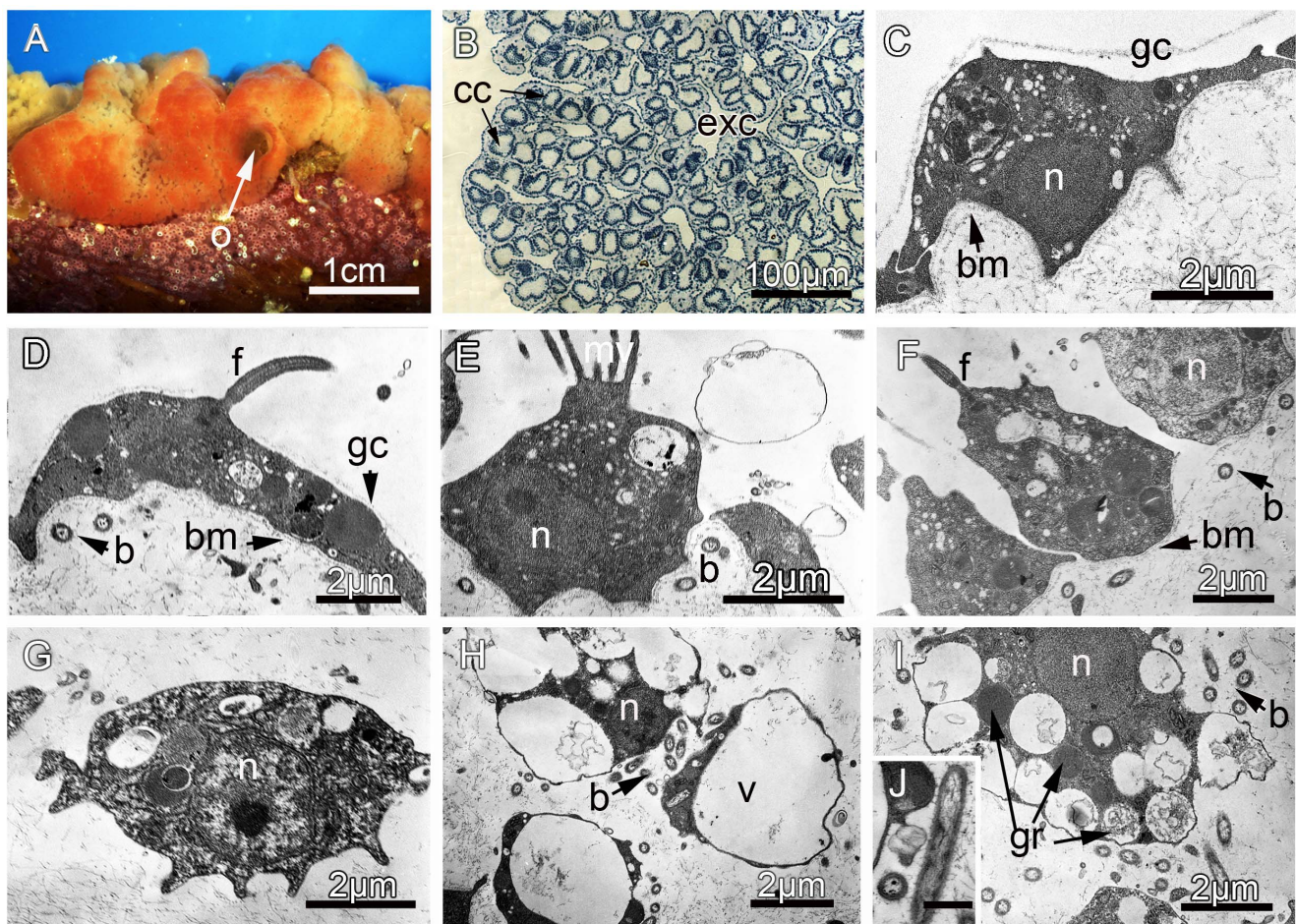


Figure 6. *Oscarella bergensis* sp. nov. (A) External morphology *in vivo*. (B) General anatomy, observed with light microscopy. (C) TEM of exopinacocyte. (D) TEM of endopinacocyte. (E) TEM of apopylar cell. (F) TEM of choanocyte. (G) TEM of archaeocyte. (H) TEM of vacuolar cells. (I) TEM of granular cells. (J) TEM of symbiotic bacteria. (b) Symbiotic bacteria; (bm) Basement membrane; (cc) Choanocyte chamber; (ec) Ectosome; (exc) Exhalant canal; (exp) Exopinacodem; (f) Flagellum; (gc) Glycocalyx; (gr) Granules; (mv) Microvilli; (n) Nucleus; (o) Osculum; (v) Vacuole. Scale bar: J = 0.5 μ m.
doi:10.1371/journal.pone.0063976.g006

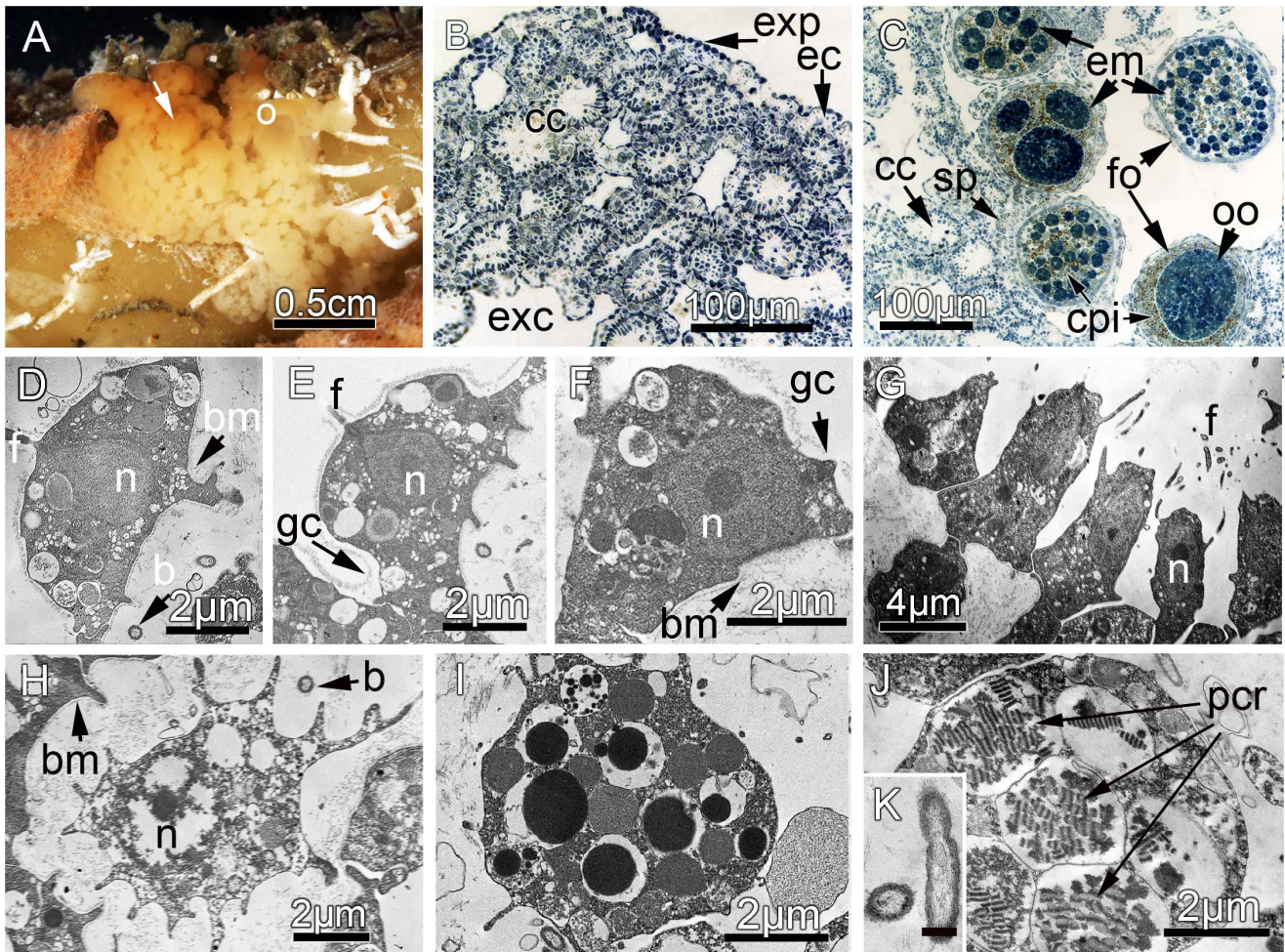


Figure 7. *Oscarella nicolae* sp. nov. (A) External morphology *in vivo*. (B) General anatomy, observed with light microscopy. (C) Light microscopy, details of hermaphrodite sponge during reproduction. (D) TEM of exopinacocyte. (E) TEM of endopinacocyte. (F) TEM of apopylar cell. (G) TEM of choanocyte. (H) TEM of archaeocyte. (I) TEM of granular cell. (J) TEM of spherulous cells with paracrystalline inclusions. (K) TEM of symbiotic bacteria. (b) Symbiotic bacteria; (bm) Basement membrane; (cc) Choanocyte chamber; (cpi) Spherulous cells with paracrystalline inclusions; (ec) Ectosome; (em) Embryos; (exc) Exhalant canal; (exp) Exopinacoderm; (f) Flagellum; (fo) Follicle; (gc) Glycocalyx; (gr) Granules; (n) Nucleus; (o) Osculum; (oo) Oocyte; (pci) Spherulous with paracrystalline inclusions; (sp) Spermatid cyst. Scale bar: J=0.5 μ m. doi:10.1371/journal.pone.0063976.g007

Discussion

1. Suitability and Limits of Molecular Markers Used

All four markers used for this study were informative for understanding phylogenetic relationships within Oscarellidae and produced mostly congruent trees (Figures 2, 3 and 4). However, some differences were observed in the performance of individual markers and are discussed below.

The 18S rDNA analyses resolved the deeper nodes of the phylogenies. The suitability of this marker for reconstructing relationships at family level has often been demonstrated in sponge phylogenies [27]. Nevertheless, as previously noticed, its power of resolution is insufficient for deciphering relationships between closely-related species: this is the case here - and was expected given our previous data - for *Oscarella tuberculata* and *O. lobularis* color morphs, and more generally within the clade D. The 28S rDNA mostly confirms the main topology obtained with the 18S rDNA but did not provide higher resolution for the D clade. Moreover, the inferred relationships within D were different between the two nuclear markers. These observed discrepancies could be explained either by scarcity of the phylogenetic signal or

by the fact that these markers constitute multigene families. Although it is generally assumed that paralogous copies of rDNA genes are homogeneous [62,63,64] because they evolve by concerted evolution, this is not always the case, and conflicting phylogenies have been inferred when using different copies of ITS [65,66] or 18S rDNA [67,68]. Nevertheless, one can suppose that the action of concerted evolution may not be sufficient to compensate paralogous evolution for recently diverged species.

Mitochondrial markers provide several advantages for phylogenetic reconstructions including their higher rate of sequence evolution and the rarity of gene duplication. Assuming the uniparental inheritance (common for most metazoans) and the effective absence of recombination (characteristic for Metazoa), the whole mtDNA should evolve as a single locus.

Thus, we selected two regions that showed the highest diversity in Oscarellidae in our preliminary results. Not surprisingly, these two regions did not include *cox1*, which is one of the most conserved regions of the mitochondrial genome and often fails to resolve relationships among closely-related sponge species [69,70] and, in general, often performs worse in resolving animal

relationships than other genes. The *atp6* marker has already been selected for alpha-level systematics in Demospongiae because it was more polymorphic than *cox1* in the studied species [38]. In our case, despite comparable nucleotide diversity (Π, Table 5), *atp6* appears not to be powerful enough to clearly resolve phylogenetic relationships among members of D clade. *TatC* is the gene that encodes the subunit C of twin-arginine translocase. The Twin-Arginine Translocation Pathway is involved in transfer of folded proteins across biological membranes in bacteria, chloroplast and, possibly, mitochondria [71]. *TatC* gene is not found in any other sponge or animal mtDNA [72,73] but is commonly present in mitochondrial genomes of other eukaryotes [74]. It was first reported in the *O. carmela* genome [73] and then found in other Oscarellidae species ([6], this study). This gene appears to be more variable than *atp6* and is the most variable of our four markers. The *tatC* marker thus helped to better resolve the D clade relationships and led us to propose the D1, D2 and D3 sub-clades. We were surprised that despite their geographical distance and cyto-morphological differences, the three samples of sub-clade D3 have identical sequences for both *tatC* and *atp6* genes. This observation suggests either the presence of three different morphotypes of only one species (see section 4.4) or the fact that both mt markers are non-resolving at this scale. The limit of resolution issue for mt markers was already known for non-bilaterian species [75]. A study at a finer scale using more variable markers (e.g. introns) will be necessary in the future to understand the evolutionary history of D3 individuals.

2. Monophyly of *Oscarella* and Synonymy with *Pseudocorticium*

Our results confirm that the Oscarellidae, i.e. the Homoscleromorpha without skeletons, are separated into two clades A and B. *Pseudocorticium jarrei* is clearly included in clade A, and this is congruent with chemical data obtained by metabolic fingerprints [8]. The species also shares with all but one *Oscarella* spp. a character of the secondary structure of the 18S rDNA V4 region (internal and terminal loop), which can be considered as diagnostic for this group. *Pseudocorticium jarrei*, however, differs from *Oscarella* spp. by the development of the mesohyl, the aquiferous system and the thickness of the cortex. Two taxonomic interpretations are possible: (i) to maintain the genus *Pseudocorticium* for clade A, with transfer of *Oscarella balibaloï*, *O. nicolae* sp. nov. and *O. kamchatkensis* to *Pseudocorticium*, (ii) to synonymize *Pseudocorticium* with *Oscarella*, with transfer of *P. jarrei* to *Oscarella*. We prefer the second alternative involving fewer changes, considering that the outer morphology, aquiferous system and development of the mesohyl of *P. jarrei* can be considered as homoplastic features [6]. We thus propose the abandonment of the genus *Pseudocorticium*, which is presently made up of only one species. *Pseudocorticium jarrei* is thus transferred to *Oscarella*. Consequently, the Oscarellidae becomes a monogeneric (*Oscarella*) family, with the following definition: Homoscleromorpha without skeletons, with a variable degree of ectosome development. The aquiferous system has a syllebid-like or leuconoid organization, with eurypylous or diplodal choanocyte chambers. Their mitochondrial genomes encode a gene absent in other animal mitochondrial genomes: *tatC* [6].

3. The Two Sibling Species *Oscarella Lobularis* and *O. tuberculata*

Our molecular results, including several color morphs for both *Oscarella lobularis* and *O. tuberculata*, mainly confirm and extend the previous study based on allozymes [12]. Indeed, phylogenetic analyses, molecular divergence and nucleotide diversity calcula-

tions suggest that *O. lobularis* and *O. tuberculata* are two different and distinct species that live in sympatry. This is also corroborated by the presence of diagnostic positions in both mt DNA markers for each species (Figure S3). Cell composition [12], symbiotic microbe diversity [21], as well as life history traits such as sex ratios and reproductive cycles, also differ between *O. lobularis* and *O. tuberculata*, consistent with the presence of two distinct species [14]. Concerning color polymorphism, the type species *O. lobularis* displays not only the classical purple/ivory color arrangement but can also be blue, pink and purple. *O. tuberculata* specimens also present a variety of colors from yellow to purple. The high polychromism observed in these two species is quite unusual, compared to other sponges, although color variability is often observed between specimens of sponges living in different local environmental conditions (shady side *vs* exposed to light) [76] and non-ecophenotypical polychromism in sponges can also be found (e.g. *Mycale* species [77]). All color morphs of both *O. lobularis* and *O. tuberculata* from our study live in the same areas and environments. A wide comparison within sponges is hampered by the fact that very few studies combining molecular and morphological data on color morphs of sponges have been conducted so far.

In several genera, it has been shown that color morphs are, in fact, distinct species: e.g. *Suberites ficus* from Great Britain using allozymes [78], or *Latrunculia* from New Zealand, using allozymes and chemical studies [79]. An almost comparable situation to what we found in *Oscarella* species is the case of *Callyspongia vaginalis*. This species has three morphotypes that vary in both color and shape, but which have identical sequences for four molecular markers, thus revealing that they all belong to the same species [80] (or that the markers do not evolve fast enough).

We cannot unequivocally exclude that each color morph (for both *O. tuberculata* and *O. lobularis*) may represent populations in the course of speciation; each might become a new species in the future. This is particularly the case of the *O. tuberculata* yellow morph, which is the most divergent in this species. In addition, these color morphs may also already be different recent species that were not discriminated by the markers used. A population genetics study using more variable markers with more specimens of various localities is needed to conclusively solve this question (assuming that “true” species exist in nature: see [81] for some insights). Nevertheless, the absence of distinguishable morphological characters between these color morphs, and particularly the fact that they are sympatric has led us now to prioritize, the polychromism hypothesis, and hence the presence of only two species.

As the homoscleromorph sponge *O. lobularis* is now emerging as a sponge model for evo-devo studies [13,22,23,24], clear criteria for sampling are indispensable. As color is not a valid diagnostic character to distinguish this sponge from *O. tuberculata*, only the *in situ* evaluation of the specimen consistency (soft *vs* cartilaginous) is useful during collection. This could be complemented by sequencing *atp6* and/or *tatC* and looking for diagnostic positions (see Figure S3) and for the presence of vacuolar cells in LM.

4. One or Several Species in sub-clade D3? An Open Question

Our results based on phylogenetic analyses, molecular divergence and nucleotide diversity calculations have revealed no divergence/diversity between *Oscarella* sp. (purple), *O. rubra* and *O.* sp. (pink) in mitochondrial sequences. However, conventional taxonomy based on morphological characters has revealed that these samples have very distinct features (such as outer morphology, cytology and microbial composition, see Tables 2 and 3).

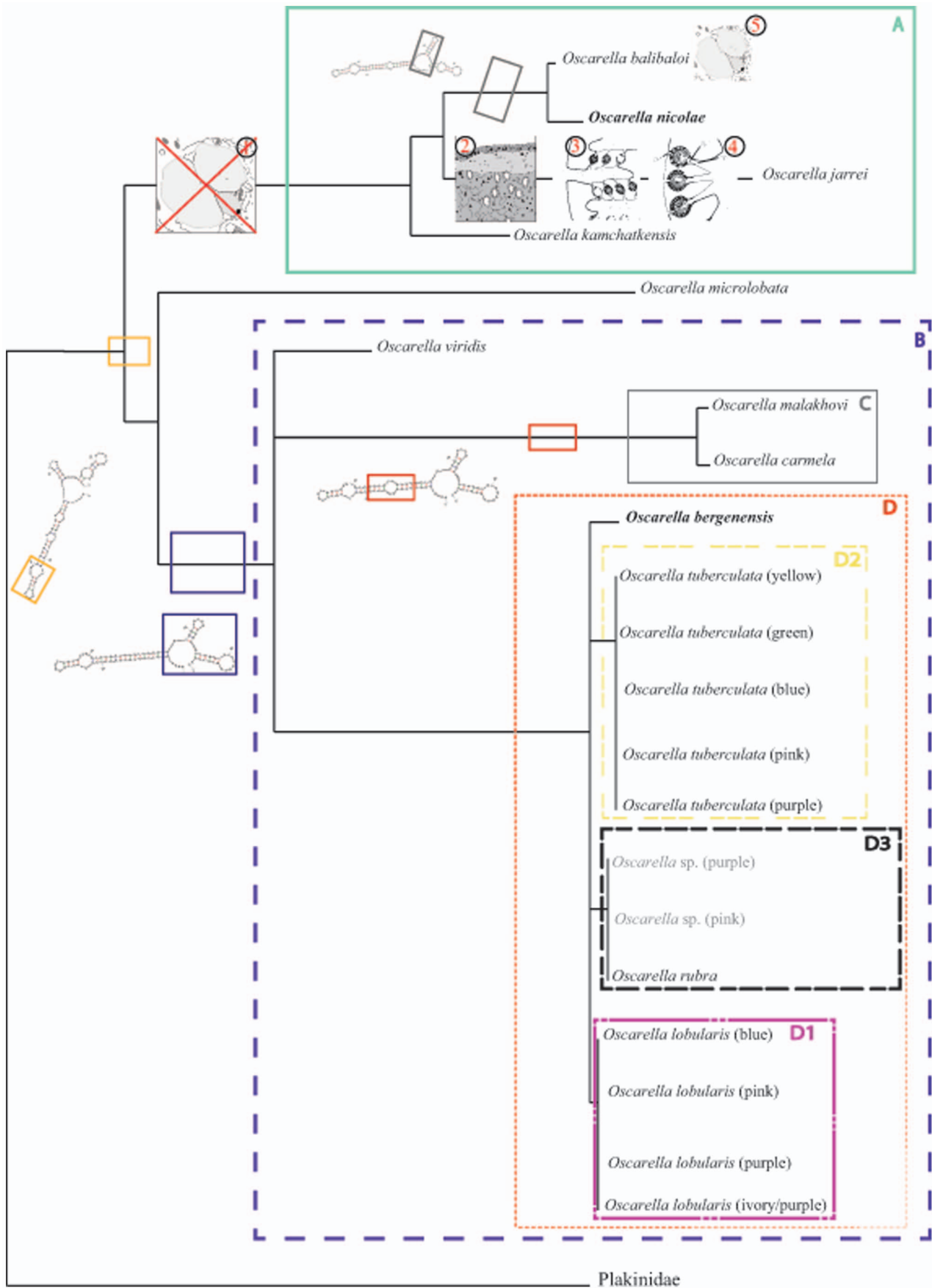


Figure 8. Simplified consensus tree based on *tatC-atp6* molecular phylogenies. All robust nodes (BP>50+ PP>0.5) were conserved. Polytoomy was prioritized for weakly-supported nodes (BP<50 or PP<0.5). Molecular and non-molecular characters that are synapomorphies/diagnostic characters of the clades are indicated on the corresponding nodes. The absence of vacuolar cells (1) is diagnostic of A. The presence of cortex (2), leuconoid aquiferous system (3) and diplodal chambers (4) are specific characters of *Oscarella jarrei*. The presence of vacuolar cells in *O. balibalo* is a reversal character (5) The two new species names are indicated in bold in the tree. In light grey are specimen/species for which uncertainties remain (new species or not). Schemas of morphological characters are modified from [60] or are new.
doi:10.1371/journal.pone.0063976.g008

These three specimens could represent a single, morphologically variable species, *Oscarella rubra*, or may represent three distinct species. This can be resolved only by a more complete study based on more numerous specimens.

5. At least Two New *Oscarella* Species from Bergen Fjords

In this study, three different species/specimens of sponge, living in sympatry and belonging to the *Oscarella* have been sampled in Bergen fjords. Molecular data, especially the mitochondrial data, have revealed that these specimens are not closely-related but belong to three distinct species. Consequently, two of them have been morphologically described and formally named (see results). *Oscarella nicolae* sp. nov. belongs to clade A and is more closely-related to *O. jarrei*, *O. kamchatkensis* and *O. balibalo* than to the other species from Bergen fjords. Its external morphology and, in particular, its microlobate surface, distinguish this species from the two others. Cytological characters are also informative: archaeocytes are often present in its mesohyl, while no vacuolar cells have been found, contrary to the two other species. Moreover, *O. nicolae* sp. nov. contains spherulous cells with paracrystalline inclusions and has no vacuolar cells as is the case for the other members of clade A. The affinity of *O. nicolae* sp. nov. with *O. balibalo* is also supported by a shared secondary structure element in their 18S rDNA. *Oscarella bergenensis* sp. nov. is included in clade D, with uncertain relationships regarding D1, D2 and D3 sub-clades. It is clearly distinct from the two other samples from Bergen, as shown by phylogenetic analyses. Furthermore, its external morphology (color and consistency) is different to the two other specimens from Bergen, while its histological and cytological features are quite similar to *Oscarella* sp. (pink). The last Bergen specimen, *Oscarella* sp. (pink) belongs to D3 sub-clade and it is unclear whether it is *O. rubra* or a new species (see 4.4). Present data are insufficient, preventing firm conclusions from being drawn, as a result, we propose no morphological description for the moment.

Conclusions

The taxonomy of sponges is usually based on the characters of the skeleton, fibers and spicules. Due to the absence of skeleton and to the presence of mainly invariable histological character-states, the identification of *Oscarella* at the species level is very difficult. The differences among species are mostly in external traits: color, consistency, and aspect of the surface [12,15,16,17,18,28,29,57], but these characters must be evaluated with care; they can be highly subjective and also very polymorphic. At the same time, some cytological characters, such as the presence of types of cells with inclusions and symbiotic microbes morphology, have been proposed to be more informative for some *Oscarella* species identification [15,16,17,18,21,29]. These findings are corroborated by the present molecular study because species previously described using morphology are confirmed here with molecular data. Nevertheless, except for two (absence of vacuolar cells and possibly spherulous cells with paracrystalline inclusions), these morphological character-states are not powerful tools for reconstructing species relationships in this group (Figure 8). Mapping morphological characters on molecular trees to identify synapomorphies which support clades has been a successful

approach for diverse groups (e.g. Demospongiae, Calcarea [2,34,82,83]) although it has also been poorly indicative or unsuccessful for some demosponge taxa: Haplosclerida, Halichondrida, Axinellidae [37,84,85,86], as well as for Oscarellidae (Figure 8). This study offers additional evidence that when there are few available morphological features to study and compare, molecular biology offers a powerful tool to provide insights into phylogenetic relationships [55], but this also requires the discovery of an efficient marker for the question under investigation. A more in-depth exploration of the microbial diversity of the species (e.g. identification of associated species rather than bacterial morphotypes) may also be a successful alternative path to follow for Oscarellidae phylogeny and systematics [87].

Supporting Information

Figure S1 Different *in situ* color morphs of *Oscarella lobularis* and *O. tuberculata* species from the Marseille area. A to D: *O. lobularis*. E to I: *O. tuberculata*.
(TIF)

Figure S2 Evolution of some Oscarellidae characters, as optimized by Mesquite on a simplified consensus tree. Double colored branches indicate non-determination of character-state in the branch. The squares below taxon names give character state in the considered taxon; no square means unknown (in this case, character-state in the corresponding branch is optimized according to character-states in related taxa). Clades A, B, C and D are indicated. (A) Characters: basement membrane, cincto-blastula larvae, multipolar ingression and asynchronous spermatogenesis. Presence in black; absence in white; (B) Character: Spherulous cells with paracrystalline inclusions. Presence in black; absence in white; (C) Characters: cortex, canal system and choanocyte chambers. Presence/leuconoid/diplodal in black; absence/sylleibid/eurypylous in white; (D) Character: vacuolar cells. Presence of two types in black; presence of one type in green; absence in white.
(EPS)

Figure S3 Molecular diagnostic positions for *Oscarella lobularis* and *O. tuberculata*. Partial alignments of mitochondrial markers (*atp6* and *tatC*) are provided and the diagnostic positions are identified by a black hexagon. A summary table for diagnostic positions for each marker for each species is also proposed.
(EPS)

Table S1 PCR primers. Names and sequences for primers used for rDNA and mitochondrial amplifications as well as references are provided.
(DOC)

Text S1 Mesquite matrix for some morphological characters from Tables 2 and 3. Characters and character-states are detailed.
(PDF)

Text S2 Mesquite matrix for V4 secondary structures for 18S rDNA.
(PDF)

Acknowledgments

We gratefully acknowledge Guilherme Muricy, Michelle Kelly, Wilfried Bay-Nouailhat, Rob van Soest and Pascal Lapébie for providing specimens and Didier Aurelle, an anonymous reviewer and the PLoS One Editor for helpful comments on the manuscript. We thank Dr Emilie Egea for her help with partitioning dataset. We are indebted to Daria Tokina for her assistance with samples preparation to LM and TEM observations. Frederic Zuberer and Marcin Adamski are thanked for diving assistance and the molecular biology staff of the IMBE laboratory (SCBM) for technical means provided.

References

- Gazave E, Lapébie P, Ereskovsky AV, Vacelet J, Renard E, et al. (2012) No longer Demospongiae: Homoscleromorpha formal nomination as a fourth class of Porifera. *Hydrobiologia* 687: 3–10.
- Borchellini C, Chombar C, Manuel M, Alivon E, Vacelet J, et al. (2004) Molecular phylogeny of Demospongiae: implications for classification and scenarios of character evolution. *Mol Phylogenet Evol* 32: 823–837.
- Dohrmann M, Janussen D, Reitner J, Collins AG, Wörheide G (2008) Phylogeny and evolution of glass sponges (Porifera, Hexactinellida). *Syst Biol* 57: 388–405.
- Dohrmann M, Voigt O, Erpenbeck D, Wörheide G (2006) Non-monophyly of most supraspecific taxa of calcareous sponges (Porifera, Calcarea) revealed by increased taxon sampling and partitioned Bayesian analysis of ribosomal DNA. *Mol Phylogenet Evol* 40: 830–843.
- Pick KS, Philippe H, Schreiber F, Erpenbeck D, Jackson DJ, et al. (2010) Improved phylogenomic taxon sampling noticeably affects nonbilaterian relationships. *Mol Biol Evol* 27: 1983–1987.
- Gazave E, Lapébie P, Renard E, Vacelet J, Rocher C, et al. (2010) Molecular phylogeny restores the supra-generic subdivision of homoscleromorph sponges (Porifera, Homoscleromorpha). *PLoS ONE* 5: e14290.
- Boury-Esnault N, Muricy G, Gallissian MF, Vacelet J (1995) Sponges without skeleton: a new Mediterranean genus of Homoscleromorpha (Porifera, Demospongiae). *Ophelia* 43: 25–43.
- Ivanisevic J, Thomas OP, Lejeune C, Chevalloné P, Pérez T (2011) Metabolic fingerprinting as an indicator of biodiversity: towards understanding inter-specific relationships among Homoscleromorpha sponges. *Metabolomics* 7: 289–304.
- Van Soest RWM, Boury-Esnault N, Hooper JNA, Rützler K, de Voogd NJ, et al. (2013) World Porifera database. Available: <http://www.marinespecies.org/porifera>.
- Schmidt O (1862) Die Spongien des Adriatischen Meeres. Leipzig: Verlag Von Wilhelm Engelmann. 88 p.
- Topsent E (1897) Spongiaires de la Baie d'Amboine. (Voyage de MM. M. Bedot et C. Pictet dans l'Archipel Malais). *Rev Suisse Zool* 4: 421–487.
- Boury-Esnault N, Sole-Cava AM, Thorpe JP (1992) Genetic and cytological divergence between colour morphs of the Mediterranean sponge *Oscarella lobularis* Schmidt (Porifera, Demospongiae, Oscarellidae). *J Nat Hist* 26: 271–284.
- Ereskovsky AV, Borchellini C, Gazave E, Ivanisevic J, Lapébie P, et al. (2009) The Homoscleromorph sponge *Oscarella lobularis*, a promising sponge model in evolutionary and developmental biology. *Bioessays* 31: 89–97.
- Ereskovsky AV, Dubois M, Ivanisevic J, Gazave E, Lapébie P, et al. (2013) Pluri-annual study of the reproduction of two Mediterranean *Oscarella* species (Porifera, Homoscleromorpha): cycle, sex-ratio, reproductive effort and phenology. *Mar Biol* 160: 423–438.
- Ereskovsky (2006) A new species of *Oscarella* (Demospongiae: Plakinidae) from the Western Sea of Japan. *Zootaxa* 1376: 37–51.
- Ereskovsky AV, Sanamayan K, Vishnyakov AE (2009) A new species of the genus *Oscarella* (Porifera: Homosclerophorida: Plakinidae) from the North-West Pacific. *Cah Biol Mar* 50: 369–381.
- Pérez T, Ivanisevic J, Dubois M, Pedel L, Thomas OP, et al. (2011) *Oscarella balibaloï*, a new sponge species (Homoscleromorpha: Plakinidae) from the Western Mediterranean Sea: cytological description, reproductive cycle and ecology. *Mar Ecol* 32: 174–187.
- Ereskovsky AV, Lavrov DV, Willenz P (2013) Five new species of Homoscleromorpha (Porifera) from the Caribbean Sea and re-description of *Plakina jamaicensis* Lehnert and van Soest, 1998. *J Mar Biol Assoc UK*.
- Lévi C (1956) Étude des *Halisarca* de Roscoff. Embryologie et systématique des démosponges. *Arch Zool Exp Gén* 93: 1–184.
- Ereskovsky AV, Lavrov DV, Boury-Esnault N, Vacelet J (2011) Molecular and morphological description of a new species of *Halisarca* (Porifera, Demospongiae: Halisarcida) from Mediterranean Sea with re-description of the type species *Halisarca dujardini*. *Zootaxa* 2768: 5–31.
- Vishnyakov AE, Ereskovsky AV (2009) Bacterial symbionts as an additional cytological marker for identification of sponges without a skeleton. *Mar Biol* 156: 1625–1632.
- Gazave E, Lapébie P, Renard E, Bezac C, Boury-Esnault N, et al. (2008) NK homeobox genes with choanocyte-specific expression in homoscleromorph sponges. *Dev Genes Evol* 218: 479–489.

Author Contributions

Conceived and designed the experiments: EG DVL ER CB AVE. Analyzed the data: EG DVL ER JV CB AVE. Wrote the paper: EG DVL ER CB AVE. Performed the molecular experiments/participated in the acquisition of molecular data (for rDNA): EG JC MA CR CB. Performed the molecular experiments/participated in the acquisition of molecular data (for mtDNA): DVL. Performed the morphological studies: AVE JV.

- Lapébie P, Gazave E, Ereskovsky A, Derelle R, Bezac C, et al. (2009) WNT/ beta-catenin signalling and epithelial patterning in the homoscleromorph sponge *Oscarella*. *PLoS ONE* 4: e5823.
- Adamski M, Degnan BM, Green K, Zwafink C (2011) What sponges can tell us about the evolution of developmental processes. *Zoology* 114: 1–10.
- Ereskovsky AV, Renard E, Borchellini C (2013) Cellular and molecular processes leading to embryo formation in sponges: evidences for high conservation of processes throughout animal evolution. *Dev Genes Evol* 223: 5–22.
- Voigt O, Erpenbeck D, Wörheide G (2008) Molecular evolution of rDNA in early diverging Metazoa: first comparative analysis and phylogenetic application of complete SSU rDNA secondary structures in Porifera. *BMC Evol Biol* 8: 69.
- Cárdenas P, Pérez T, Boury-Esnault N (2012) Sponge Systematics facing new challenges. *Advanc Mar Biol* 61: 79–209.
- Bergquist P, Kelly M (2004) Taxonomy of some Halisarcida and Homosclerophorida (Porifera: Demospongiae) from the Indo-Pacific. *New Zeal J Mar Freshwat Res* 38: 51–66.
- Muricy G, Pearse JS (2004) A new species of *Oscarella* (Demospongiae: Plakinidae) from California. *Proc California Acad Sci* 55: 598–612.
- Muricy G, Boury-Esnault N, Bézac C, Vacelet J (1996) Cytological evidence for cryptic speciation in Mediterranean *Oscarella* species (Porifera, Homoscleromorpha). *Can J Zool* 74: 881–896.
- Ereskovsky AV, Konjukov P, Willenz P (2007) Experimental metamorphosis of *Halisarca dujardini* larvae (Demospongiae, Halisarcida): Evidence of flagellated cell totipotentiality. *J Morph* 265: 529–536.
- Maddison WP, Maddison DR (2010) Mesquite: a modular system for evolutionary analysis. Version 2.73. Available: <http://mesquiteproject.org>.
- Borchellini C, Manuel M, Alivon E, Boury-Esnault N, Vacelet J, et al. (2001) Sponge paraphyly and the origin of Metazoa. *J Evol Biol* 14: 171–179.
- Manuel M, Borchellini C, Alivon E, Le Parco Y, Vacelet J, et al. (2003) Phylogeny and evolution of calcareous sponges: monophyly of Calcinea and Calcarea, high level of morphological homoplasy, and the primitive nature of axial symmetry. *Syst Biol* 52: 311–333.
- Blanquer A, Uriz MJ (2007) Cryptic speciation in marine sponges evidenced by mitochondrial and nuclear genes: a phylogenetic approach. *Mol Phylogenet Evol* 45: 392–397.
- Kelly-Borges M, Pomponi S (1994) Phylogeny and classification of lithistid sponges (Porifera: Demospongiae): a preliminary assessment using ribosomal DNA sequence comparisons. *Mol Mar Biol Biotechnol* 3: 87–103.
- Gazave E, Carteron S, Chenail A, Richelle-Maurer E, Boury-Esnault N, et al. (2010) Polyphyly of the genus *Axinella* and of the family Axinellidae (Porifera: Demospongiae). *Mol Phylogenet Evol* 57: 35–47.
- Rua CPJ, Zilberberg C, Solé-Cava A (2011) New polymorphic mitochondrial markers for sponge phylogeography. *J Mar Biol Ass UK* 91: 1015–1022.
- Solé-Cava AM, Wörheide G (2007) The perils and merits (or the Good, the Bad and the Ugly) of DNA barcoding of sponges – a controversial discussion. In: M.R. Custódio GL-H, E Hajdu, G Muricy, editor. *Porifera Research: Biodiversity, Innovation and Sustainability*. Rio de Janeiro: Museu Nacional. 603–612.
- Altschul SF, Gish W, Miller W, Myers EW, Lipman DJ (1990) Basic local alignment search tool. *J Mol Biol* 215: 403–410.
- Edgar RC (2004) MUSCLE: a multiple sequence alignment method with reduced time and space complexity. *BMC Bioinformatics* 5: 113.
- Edgar RC (2004) MUSCLE: multiple sequence alignment with high accuracy and high throughput. *Nucleic Acids Res* 32: 1792–1797.
- Hall TA (1998) Bioedit: a user-friendly biological sequence alignment editor and analysis program for Windows 95/98/NT. *Nucleic Acids Symp Ser* 41: 95–98.
- Castresana J (2000) Selection of conserved blocks from multiple alignments for their use in phylogenetic analysis. *Mol Biol Evol* 17: 540–552.
- Talavera G, Castresana J (2007) Improvement of phylogenies after removing divergent and ambiguously aligned blocks from protein sequence alignments. *Syst Biol* 56: 564–577.
- Posada D (2008) jModelTest: phylogenetic model averaging. *Mol Biol Evol* 25: 1253–1256.
- Guindon S, Gascuel O (2003) A simple, fast, and accurate algorithm to estimate large phylogenies by maximum likelihood. *Syst Biol* 52: 696–704.

48. Guindon S, Lethiec F, Duroux P, Gascuel O (2005) PHYML Online—a web server for fast maximum likelihood-based phylogenetic inference. *Nucleic Acids Res* 33: W557–559.
49. Felsenstein J (1985) Confidence limits on phylogenies: an approach using the bootstrap. *Evolution* 39: 783–791.
50. Ronquist F, Huelsenbeck JP (2003) MrBayes 3: Bayesian phylogenetic inference under mixed models. *Bioinformatics* 19: 1572–1574.
51. Nylander JA (2004) MrModeltest v2. Program distributed by the author. Evolutionary Biology Centre, Uppsala University.
52. Rambaut A (2010) FigTree 1.3.1. Available: <http://treebioedacuk/software/figtree/>.
53. Zuker M (2003) Mfold web server for nucleic acid folding and hybridization prediction. *Nucleic Acids Res* 31: 3406–3415.
54. Wuyts J, Van de Peer Y, Winkelmans T, De Wachter R (2002) The European database on small subunit ribosomal RNA. *Nucleic Acids Res* 30: 183–185.
55. Redmond NE, McCormack GP (2008) Large expansion segments in 18S rDNA support a new sponge clade (Class Demospongiae, Order Haplosclerida). *Mol Phylogenet Evol* 47: 1090–1099.
56. Librado P, Rozas J (2009) DnaSP v5: a software for comprehensive analysis of DNA polymorphism data. *Bioinformatics* 25: 1451–1452.
57. Muricy G, Diaz MC (2002) Order Homosclerophorida Dendy, 1905, Family Plakinidae Schulze, 1880. In: Hooper JNA, Van Soest RWM, editors. *Systema Porifera: A Guide to the Classification of Sponges*. New-York: Kluwer Academic/Plenum Publishers. 71–82.
58. Hanitsch R (1890) Third report on the Porifera of the L.M.B.C. District. *Trans Liverpool Biol Soc.* 192–238.
59. Muricy G, Solé Cava AM, Thorpe JP, Boury-Esnault N (1996) Genetic evidence for extensive cryptic speciation in the subtidal sponge *Plakina trilopha* (Porifera: Demospongiae: Homoscleromorpha) from the Western Mediterranean. *Mar Ecol Progr* 138: 181–187.
60. Boury-Esnault N, Rützler K, editors (1997) *Thesaurus of Sponge Morphology*. Washington, D.C.: Smithsonian Institution Press.
61. Muricy G, Boury-Esnault N, Bézac C, Vacelet J (1998) Taxonomic revision of the Mediterranean *Plakina* Schulze (Porifera, Demospongiae, Homoscleromorpha). *Zool J Linn Soc* 124: 169–203.
62. Hillis DM, Dixon MT (1991) Ribosomal DNA: molecular evolution and phylogenetic inference. *Q Rev Biol* 66: 411–453.
63. Dover G (1982) Molecular drive: a cohesive mode of species evolution. *Nature* 299: 111–117.
64. Arnheim N, Krystal M, Schmickel R, Wilson G, Ryder O, et al. (1980) Molecular evidence for genetic exchanges among ribosomal genes on nonhomologous chromosomes in man and apes. *Proc Natl Acad Sci U S A* 77: 7323–7327.
65. Li C, Wilkerson RC (2007) Intra-genomic rDNA ITS2 variation in the neotropical *Anopheles* (Nyssorhynchus) *albiparis* complex (Diptera: Culicidae). *J Hered* 98: 51–59.
66. Calderon I, Garrabou J, Aurelle D (2006) Evaluation of the utility of COI and ITS markers as tools for population genetic studies of temperate gorgonians. *J Exper Mar Biol Ecol* 336: 184–197.
67. Carranza S, Giribet G, Ribera C, Baguna, Riutort M (1996) Evidence that two types of 18S rDNA coexist in the genome of *Dugesia* (*Schmidtea*) *mediterranea* (Platyhelminthes, Turbellaria, Tricladida). *Mol Biol Evol* 13: 824–832.
68. Muir G, Fleming CC, Schlotterer C (2001) Three divergent rDNA clusters predate the species divergence in *Quercus petraea* (Matt.) Liebl. and *Quercus robur* L. *Mol Biol Evol* 18: 112–119.
69. Duran S, Giribet G, Turon X (2004) Phylogeographical history of the sponge *Crambe crambe* (Porifera, Poecilosclerida): range expansion and recent invasion of the Macaronesian islands from the Mediterranean Sea. *Mol Ecol* 13: 109–122.
70. Wörheide G (2006) Low variation in partial cytochrome oxidase subunit I (COI) mitochondrial sequences in the coralline demosponge *Astroclera willelyana* across the Indo-Pacific. *Mar Biol* 148: 907–912.
71. Palmer T, Berks BC (2012) The twin-arginine translocation (Tat) protein export pathway. *Nat Rev Microbiol* 10: 483–496.
72. Lavrov DV, Wang X, Kelly M (2008) Reconstructing ordinal relationships in the Demospongiae using mitochondrial genomic data. *Mol Phylogenet Evol* 49: 111–124.
73. Wang X, Lavrov DV (2007) Mitochondrial genome of the homoscleromorph *Oscarella carmela* (Porifera, Demospongiae) reveals unexpected complexity in the common ancestor of sponges and other animals. *Mol Biol Evol* 24: 363–373.
74. Yen MR, Tseng YH, Nguyen EH, Wu LF, Saier MH Jr (2002) Sequence and phylogenetic analyses of the twin-arginine targeting (Tat) protein export system. *Arch Microbiol* 177: 441–450.
75. Huang D, Meier R, Todd PA, Chou LM (2008) Slow mitochondrial COI sequence evolution at the base of the metazoan tree and its implications for DNA barcoding. *J Mol Evol* 66: 167–174.
76. Cook SdC, Bergquist PR (2002) Family Spongiidae Gray, 1867. In: Hooper JNASRWMv, editor. *Systema Porifera: A guide to the classification of Sponges*. New York: Kluwer Academic/Plenum Publishers. 1051–1060.
77. Hajdu E, Rützler K (1998) Sponges, genus *Mycale* (Poecilosclerida: Demospongiae: Porifera), from a Caribbean mangrove and comments on subgeneric classification. *Proc Biol Soc Washington* 111: 737–773.
78. Solé-Cava AM, Thorpe JP (1986) Genetic differentiation between morphotypes of the marine sponge *Suberites ficus* (Demospongiae: Hadromerida). *Mar Biol* 93: 247–253.
79. Miller K, Alvarez B, Battershill C, Northcote P, Parthasarathy H (2001) Genetic, morphological, and chemical divergence in the sponge genus *Latrunculia* (Porifera: Demospongiae) from New Zealand. *Mar Biol* 139: 235–250.
80. López-Legentil S, Erwin PM, Henkel TP, Loh T-L, Pawlik JR (2010) Phenotypic plasticity in the Caribbean sponge *Callyspongia vaginalis* (Porifera: Haplosclerida). *Scientia Mar* 74: 445–453.
81. Hey J, Pinho C (2012) Population genetics and objectivity in species diagnosis. *Evolution* 66: 1413–1429.
82. Chombard C, Boury-Esnault N, Tillier S (1998) Reassessment of homology of morphological characters in tetractinellid sponges based on molecular data. *Syst Biol* 47: 351–366.
83. Cárdenas P, Rapp HT, Schander C, Tender OS (2010) Molecular taxonomy and phylogeny of the Geodiidae (Porifera, Demospongiae, Astrophorida) - combining phylogenetic and Linnaean classification. *Zool Scr* 39: 89–106.
84. Alvarez B, Crisp MD, Driver F, Hooper JN, Soest RWMV (2000) Phylogenetic relationships of the family Axinellidae (Porifera: Demospongiae) using morphological and molecular data. *Zool Scr* 29: 169–198.
85. McCormack GP, Erpenbeck D, Van Soest RWM (2002) Major discrepancy between phylogenetic hypotheses based on molecular and morphological criteria within the Order Haplosclerida (Phylum Porifera: Class Demospongiae). *J Zool Systemat Evol Res* 40: 237–240.
86. Redmond NE, van Soest RW, Kelly M, Raleigh J, Travers SA, et al. (2007) Reassessment of the classification of the Order Haplosclerida (Class Demospongiae, Phylum Porifera) using 18S rRNA gene sequence data. *Mol Phylogenet Evol* 43: 344–352.
87. Gloeckner V, Hentschel U, Ereskovsky AV, Schmitt S (2013) Unique and specie-specific microbial communities in *Oscarella lobularis* and other Mediterranean *Oscarella* species (Porifera: Homoscleromorpha). *Mar Biol* 160: 781–791.
88. Schmidt O (1870) *Grundzüge einer Spongien-Fauna des atlantischen Gebietes*. Leipzig: Wilhelm Engelmann. 88 p.
89. Hooper JN, Van Soest RWM, Debrenne F (2002) Phylum Porifera Grant, 1836; *Systema Porifera: A Guide to the classification of Sponges*. In: Hooper JN, Van Soest RWM, editors. *Systema Porifera: A Guide to the classification of Sponges*. New York: Kluwer Academic/Plenum Publishers. 9–13.